


# Intercalibration of Mg Isotope Delta Scales and Realisation of SI Traceability for Mg Isotope Amount Ratios and Isotope Delta Values

Jochen Vogl (1)\* , Martin Rosner (2), Simone A. Kasemann (3), Rebecca Kraft (4), Anette Meixner (3), Janine Noordmann (5), Savelas Rabb (4), Olaf Rienitz (5), Jan A. Schuessler (6), Michael Tatzel (1) and Robert D. Vocke (4)

(1) Bundesanstalt für Materialforschung und -prüfung (BAM), Richard-Willstätter-Straße 11, Berlin, 12489, Germany

(2) IsoAnalysis UG, Gustav-Müller-Straße 38, Berlin, 10829, Germany

(3) Faculty of Geosciences & MARUM – Center for Marine Environmental Sciences, University of Bremen, Leobener Straße 8, Bremen, 28359, Germany

(4) Chemical Sciences Division, National Institute of Standards and Technology (NIST), Gaithersburg, MD, 20899, USA

(5) Physikalisch-Technische Bundesanstalt (PTB), Bundesallee 100, Braunschweig, 38116, Germany

(6) GFZ German Research Centre for Geosciences, Telegrafenberg, Potsdam, 14473, Germany

(7) Present address: Thermo Fisher Scientific GmbH, Bremen, 28199, Germany

(8) Present address: Department of Earth and Planetary Sciences, University of California Santa Cruz, 1156 High Street, Santa Cruz, CA, 95064, USA

\* Corresponding author. e-mail: jochen.vogl@bam.de

The continuous improvement of analytical procedures using multi-collector technologies in ICP-mass spectrometry has led to an increased demand for isotope standards with improved homogeneity and reduced measurement uncertainty. For magnesium, this has led to a variety of available standards with different quality levels ranging from artefact standards to isotope reference materials certified for absolute isotope ratios. This required an intercalibration of all standards and reference materials, which we present in this interlaboratory comparison study. The materials Cambridge1, DSM3, ERM-AE143, ERM-AE144, ERM-AE145, IRMM-009 and NIST SRM 980 were cross-calibrated with expanded measurement uncertainties (95% confidence level) of less than 0.030‰ for the  $\delta^{25/24}\text{Mg}$  values and less than 0.037‰ for the  $\delta^{26/24}\text{Mg}$  values. Thus, comparability of all magnesium isotope delta ( $\delta$ ) measurements based on these standards and reference materials is established. Further, ERM-AE143 anchors all magnesium  $\delta$ -scales to absolute isotope ratios and therefore establishes SI traceability, here traceability to the SI base unit mole. This applies especially to the DSM3 scale, which is proposed to be maintained. With ERM-AE144 and ERM-AE145, which are product and educt of a sublimation–condensation process, for the first time a set of isotope reference materials is available with a published value for the apparent triple isotope fractionation exponent  $\theta_{\text{app}}$ , the fractionation relationship  $\ln \alpha^{(25/24)\text{Mg}}/\ln \alpha^{(26/24)\text{Mg}}$ .

Keywords: delta scale, traceability, scale anchor, absolute isotope ratio, comparability, triple isotope fractionation.

Received 17 Jan 20 – Accepted 29 Mar 20

Isotope ratios of stable isotope systems are often reported using so-called  $\delta$ -scales. In the best case, like for lithium and boron, these  $\delta$ -scales are based on isotope reference materials (IRM) certified for their isotope amount ratios and thus enabling traceability to the SI. For most other elements, however, the  $\delta$ -scales are based on artefact standards (see Appendix S1), most commonly represented by commercial mono-elemental solutions without any traceability. Magnesium isotope ratios, for example, are typically reported as  $\delta^{26/24}\text{Mg}$  (and  $\delta^{25/24}\text{Mg}$ ) values that represent

the relative difference between the  $^{26}\text{Mg}/^{24}\text{Mg}$  (and the  $^{25}\text{Mg}/^{24}\text{Mg}$ ) ratio measured in a sample relative to its measurement in an internationally accepted standard. In the past, such  $\delta^{26/24}\text{Mg}$  (and  $\delta^{25/24}\text{Mg}$ ) measurements were referenced to the IRM NIST SRM 980, the anchor and zero point of the  $\delta^{26/24}\text{Mg}$  (and  $\delta^{25/24}\text{Mg}$ ) scale at that time. With the development of multi-collector inductively coupled plasma-mass spectrometry (MC-ICP-MS), a magnesium isotope ratio precision in the range of 0.1‰ could be achieved (e.g., Galy *et al.* 2003, Bolou-Bi *et al.* 2009, Teng

doi: 10.1111/ggr.12327

© 2020 The Authors. *Geostandards and Geoanalytical Research* © 2020 International Association of Geoanalysts

This is an open access article under the terms of the Creative Commons Attribution License,

which permits use, distribution and reproduction in any medium, provided the original work is properly cited.

*et al.* 2015), and thus, the detection of small but measurable isotopic differences in different chips of NIST SRM 980 became apparent (Galy *et al.* 2003). Although still covered by the expanded uncertainty of NIST SRM 980, these differences of 0.69‰ ( $2 \times$  standard deviation of the mean,  $2s_m$ ) were considered to be too large for current magnesium isotope research and a replacement for NIST SRM 980 was proposed (Galy *et al.* 2003, Vogl *et al.* 2004). To avoid such heterogeneity issues with solid iRMs, the community introduced two new artefact standards for Mg  $\delta$ -scale measurements. Both were pure Mg standard solutions, the first of which was DSM3, which was suggested to serve as the new  $\delta = 0$  material of the Mg  $\delta$ -scale and the second was Cambridge1, which was supposed to serve as a  $\delta$ -offset material for quality control (Galy *et al.* 2003). As both artefact standards do not provide isotope amount ratios nor fulfil most of the requirements for an iRM such as availability, traceability or uncertainty statement, there was still a pressing need for at least one new SI-traceable magnesium iRM (Vogl *et al.* 2013). Despite these metrological disadvantages, DSM3 is the currently accepted  $\delta$ -scale with its anchor point DSM3 as recognised by IUPAC (Brandt *et al.* 2014).

The traceability problem has been solved in a recent project (Brandt *et al.* 2016, Vogl *et al.* 2016) within which a series of three magnesium iRMs (European Reference Materials ERM-AE143, ERM-AE144 and ERM-AE145) has been produced, which are certified for their magnesium isotope amount ratios being traceable to the SI in the most direct way. ERM-AE143 is a potential replacement for DSM3 for anchoring the  $\delta^{26/24}\text{Mg}$  scale fulfilling all requirements for an iRM. Not to waste the past efforts and to establish comparability between  $\delta^{26/24}\text{Mg}$  values obtained via different  $\delta$ -standards, an intercalibration of all existing iRMs and artefact standards was required. We realised this in the present interlaboratory comparison study for Mg isotope ratios, within which all currently available Mg iRMs and artefact standards with natural-like Mg isotopic composition were analysed in order to establish comparability of Mg  $\delta$ -scales obtained by different  $\delta$ -materials. As the study includes SI-traceable Mg iRMs with sufficiently low measurement uncertainties, the calculation of Mg isotope amount ratios with associated measurement uncertainties for DSM3 and Cambridge1 was possible for the first time based on a fully calibrated approach.

## Materials and methods

### Isotope reference materials and artefact standards

**NIST SRM 980:** One unit of NIST SRM 980 was purchased in 2013, which contains 0.25 g of high purity

magnesium, supplied as metal chips. The certified values and further details can be obtained from the certificate (NIST 1967). At BAM, an exactly weighed amount of approximately 26 mg was dissolved in nitric acid to obtain the parent solution.

**IRMM-009:** IRMM-009 is a dissolution of one or more units of NIST SRM 980 and comes in flame-sealed quartz ampoules. Each unit contains  $\approx 4$  ml of the acidified ( $0.2 \text{ mol l}^{-1} \text{ HNO}_3$ ) magnesium solution at a magnesium mass fraction of  $\approx 32 \text{ mg kg}^{-1}$ . The certified values and further details can be obtained from the certificate (IRMM 2018). Several units of this material were purchased by BAM more than 10 years ago, three of them were used to prepare a sufficient amount of solution for this study.

**ERM-AE143:** The base material for ERM-AE143 was a compact magnesium material from Alfa Aesar ('Mg Rod', LOT: G27R008), with a purity of  $\geq 0.998 \text{ kg kg}^{-1}$ . At BAM, the material's surface was cleaned with a mixture of ethanol, hydrochloric and nitric acid and then dissolved in nitric acid. More details on the preparation of the parent solution can be obtained from Vogl *et al.* (2016). The certified values and further details can be obtained from the certificate (BAM 2018a).

**ERM-AE144:** The base material is sourced from Alfa Aesar, 'Magnesium, turnings, 99+%' (order number L08120, 100 g, LOT 10146809) with a purity of  $\geq 0.999 \text{ kg kg}^{-1}$ . This material was not surface cleaned but instead it was fed into the parent solution as-is at BAM. More details on the preparation of the parent solution can be obtained from Vogl *et al.* (2016). The certified values and further details can be obtained from the certificate (BAM 2018b).

**ERM-AE145:** The base material of ERM-AE145 was prepared at BAM using high-vacuum sublimation from the base material of ERM-AE144. Approximately 184 mg was sublimated in two rounds at approximately 520 °C sublimation temperature inside the crucible, yielding approximately 178 mg of purified material. The whole sublimated material was used for preparing the parent solution without etching. More details on the sublimation can be obtained from Brandt *et al.* (2016), more details on the preparation of the parent solution from Vogl *et al.* (2016). The certified values and further details can be obtained from the certificate (BAM 2018c).

**DSM3:** This magnesium solution was produced from pure magnesium metal (Dead Sea Magnesium Ltd., Israel) by dissolving  $\approx 10$  g in 1 l of  $0.3 \text{ mol l}^{-1}$  nitric acid at Cambridge University, UK (Galy *et al.* 2003). For this

intercomparison study, three different batches labelled 'T', 'P' and 'I' could be obtained from Jerome Chmeleff (Geosciences Environment Toulouse), Jan Schuessler (GFZ German Research Centre for Geosciences Potsdam) and Ludwik Halicz (Geological Survey of Israel). DSM3-T was distributed to all participants, whereas DSM3-P was analysed only at BAM and GFZ; DSM3-I was analysed only at BAM.

**Cambridge1:** This magnesium solution was produced from batch number T432399 of the PrimAg<sup>®</sup>-extra certified reference material from Romil Ltd., Cambridge, UK (Galy *et al.* 2003). For this comparison, two different batches labelled 'CAM1-T' and 'CAM1-P' were obtained from Jerome Chmeleff (Geosciences Environment Toulouse) and Jan Schuessler (GFZ German Research Centre for Geosciences Potsdam). CAM1-T was distributed to all participants in the comparison, whereas CAM1-P was analysed only at BAM and GFZ.

The parent solutions of the above-listed materials were all prepared using the same nitric acid and the same high purity water. They were subsequently diluted to yield a magnesium mass fraction of 2.0 mg kg<sup>-1</sup> and a nitric acid mass fraction of 20 g kg<sup>-1</sup>. These dilute solutions were filled in pre-cleaned PFA bottles and sent to all participants of this intercomparison study.

## Rationale and intercomparison design

This study was initiated to provide a robust Mg isotope data set, which allows the intercalibration of iRMs (NIST SRM 980, IRMM-009, ERM-AE143, ERM-AE144, ERM-AE145) and artefact standards (DSM3, Cambridge1) currently in use. Both Mg  $\delta$ -values, that is,  $\delta^{25/24}\text{Mg}$  and  $\delta^{26/24}\text{Mg}$ , were determined by standard-sample bracketing (SSB) against ERM-AE143 during mass spectrometric measurements. This strategy will allow the recalculation of  $\delta$ -values measured on one  $\delta$ -scale, for example, relative to DSM3, to another scale, that is, relative to another reference material used as  $\delta$ -zero material like ERM-AE143, and *vice versa*. The use of ERM-AE143 as the primary calibration material enables the calculation of SI-traceable Mg isotope amount ratios for all Mg iRMs and artefact standards in this study, but also for any other material used in future studies.

In total, five experienced institutes, namely the Bundesanstalt für Materialforschung und -prüfung (BAM), the German Research Centre for Geosciences (GFZ), the National Institute for Standards and Technology (NIST), the Physikalisch-Technische Bundesanstalt (PTB) and the University of Bremen (UBR) contributed to the here reported intercomparison study. All participants used MC-ICP-MS and ERM-AE143 as the bracketing standard, as ERM-AE143 is

the best-characterised iRM for Mg with respect to SI traceability and absolute isotope ratios. Each laboratory was instructed to provide at least nine  $\delta^{25/24}\text{Mg}$  and  $\delta^{26/24}\text{Mg}$  values for each material determined in three or four independent measurement sessions. In parallel, three different batches of DSM3 were analysed to allow the assessment of the isotopic homogeneity of DSM3.

## Calculation of Mg isotope $\delta$ -values and conversion to another scale

Determination of isotope  $\delta$ -values as defined above is commonly used when higher precision is desired than achievable in absolute isotope ratio determination. When the SSB approach is applied, a Mg isotope  $\delta$ -value can be calculated according to Equation (1). The isotope  $\delta$ -value is obtained by averaging the preceding and following standards of each sample in a measurement sequence and calculating the isotope  $\delta$ -value of the sample according to Equation (1), with  $\bar{R}$  being the mean ratio of the preceding and the following standard, here for example ERM-AE143:

$$\delta^{i/24}\text{Mg}_{\text{ERM-AE143}} = \left( \frac{R_{\text{smp}}^{\text{meas}} \left( \frac{{}^i\text{Mg}}{{}^{24}\text{Mg}} \right)}{\bar{R}_{\text{ERM-AE143}}^{\text{meas}} \left( \frac{{}^i\text{Mg}}{{}^{24}\text{Mg}} \right)} \right) - 1 \quad (1)$$

where  $i = 25, 26$ . The proper scientific notation would be  $\delta_{\text{ERM-AE143}}^{i/24}\text{Mg}$ . However, we use the traditional short form, which has been in use for more than 60 years, to avoid clutter in mathematical expressions.

When it is desired to convert a  $\delta$ -value measured against one specific standard to a  $\delta$ -value versus another standard or sample, a simple addition or subtraction of two  $\delta$ -values does not provide accurate results, because  $\delta$ -scale equations are not linear. For small  $\delta$ -values that are close to the origin of the chosen  $\delta$ -scale, using a simple linear conversion introduces only small bias, but with increasing  $\delta$ -values the bias increases and might become significant considering the achievable measurement uncertainty. In the following, the exact mathematical equations are displayed for converting  $\delta$ -values.

When a  $\delta$ -value of sample  $x$  is being measured against standard  $y$ ,  $\delta^{i/24}\text{Mg}(x)_y$ , the  $\delta$ -value of sample  $y$  against standard  $x$ ,  $\delta^{i/24}\text{Mg}(y)_x$ , can be easily calculated by Equation (2). We note that simply reverting the sign is inappropriate.

$$\delta^{i/24}\text{Mg}(y)_x = - \frac{\delta^{i/24}\text{Mg}(x)_y}{\delta^{i/24}\text{Mg}(x)_y + 1} \quad (2)$$

In case the  $\delta$ -value of sample  $x$  measured against standard  $y$  should be converted to standard  $z$ , the  $\delta$ -value of

standard  $y$  versus standard  $z$  need to be known. Then, the  $\delta$ -value of sample  $x$  versus standard  $z$  can be calculated according to Equation (3):

$$\delta^{i/24}\text{Mg}(x)_z = \delta^{i/24}\text{Mg}(x)_y \times \delta^{i/24}\text{Mg}(y)_z + \delta^{i/24}\text{Mg}(x)_y + \delta^{i/24}\text{Mg}(y)_z \quad (3)$$

Note, that in Equations (2, 3),  $\delta$ -values resulting from Equation (1) have to be entered (not per mil values). When  $\delta$ -values in per mil are to be used, they have to be divided by 1000 before they are entered into Equations (2, 3).

### Applied analytical procedures

**Analytical procedure applied at BAM:** A similar set-up and experimental conditions (as described in Vogl *et al.* 2016) for isotope amount ratio measurements were used; instrumental parameters for the applied MC-ICP-MS (Thermo Scientific Neptune Plus, Bremen, Germany) are listed in Table 1. Within this project, however,  $\delta$ -measurements were required and no absolute isotope ratio measurements; hence, some modifications were necessary. The Mg mass fraction in the solutions measured was reduced from 2 to 0.25 mg kg<sup>-1</sup>. Consequently, the typical repeatability of a MC-ICP-MS measurement was increased from < 0.005% (Vogl *et al.* 2016) to approximately 0.008% in this study. As common in  $\delta$ -measurements, the SSB approach was applied, with a blank measurement before each standard and before each sample. Each iRM and each artefact standard were measured four times in each of the three sequences in random order. Typical drift in the <sup>26</sup>Mg/<sup>24</sup>Mg ratio was 0.13‰ h<sup>-1</sup> as observed by the regular measurements of the bracketing standard ERM-AE143 during the sequences. Each sample was measured with fifty cycles, and outliers were identified based on the twofold standard deviation (2s) criterion and removed from the data. Blank correction for the outlier-corrected intensities was performed by subtracting the mean intensities from the preceding and the succeeding blank. Up to this point, calculations and corrections were made within the measurement sequence by the Thermo Scientific Neptune software. The resulting means and standard deviations were collected and copied into an Excel file for further calculations.  $\delta$ -values were obtained by averaging the preceding and following standard of each sample measurement and calculating the  $\delta$ -value of the sample according to Equation (1), with  $\bar{R}$  being the mean ratio of the preceding and the succeeding standard.

The measurement procedure was then tested for potential sources leading to a bias in the  $\delta$ -measurements.

Interferences could be easily excluded as a source for bias, because only pure Mg solutions were measured. This excludes doubly charged Ca or Ti species and any carbon-based interferences beyond the typical level in dilute nitric acid. MgH species could be excluded as well as shown by Vogl *et al.* (2016). A mismatch between standard and sample in the Mg mass fraction was reported to potentially create a bias in Mg  $\delta$ -measurements with the IsoProbe and the Nu plasma MC-ICP-MS instruments (Teng and Yang 2014). This was tested by measuring ERM-AE143 solutions in duplicate with Mg mass fractions from 0.10 mg kg<sup>-1</sup> up to 0.40 mg kg<sup>-1</sup> versus an ERM-AE143 solution at a fixed Mg mass fraction of 0.25 mg kg<sup>-1</sup>. The resulting  $\delta^{26/24}\text{Mg}$  values are all below 0.06‰, which in most cases are already covered by the repeatability at the 1s level, with a minimum  $\delta^{26/24}\text{Mg}$  value of 0.007‰ for the completely matched solution at 0.25 mg kg<sup>-1</sup>. Thus, even a mismatch of  $\pm 50\%$  in the Mg mass fraction did not lead to a bias beyond the repeatability for our set-up. More important, however, is an equal level of the nitric acid mass fraction in sample and standard as differences might lead to a different blank mobilisation or different nebulisation behaviour for sample and standard, respectively. This was tested for ERM-AE143 solutions with nitric acid mass fractions ranging from 10 to 60 g kg<sup>-1</sup>, while the Mg mass fraction were kept constant at 0.25 mg kg<sup>-1</sup>; the nitric acid mass fraction of the ERM-AE143 solution used as the standard was 20 g kg<sup>-1</sup> and the Mg mass fraction was 0.25 mg kg<sup>-1</sup>. An absolute difference in the nitric acid mass fraction of  $\pm 10$  g kg<sup>-1</sup> may lead to a bias in the  $\delta^{26/24}\text{Mg}$  value of 0.1–0.2‰. The most extreme bias of approximately 0.9‰ was observed for the ERM-AE143 sample solution measured at a nitric acid mass fraction of 60 g kg<sup>-1</sup>, while the ERM-AE143 standard solution was measured at a nitric acid mass fraction of 20 g kg<sup>-1</sup>. This agrees with the findings of Teng and Yang (2014), although the extent of the bias is significantly lower in our study. To minimise any bias by differences in sample and standard composition, all samples and standards were diluted using the same nitric acid stock solution and all samples and standards were ‘concentration’-matched to within  $\pm 10\%$  following a preceding screening of the Mg mass fractions using the MC-ICP-MS.

Measurement uncertainties were calculated based on an approach invented by Rosner *et al.* (2011), which applies a modified  $\delta$ -equation for TIMS measurements. This approach was further improved for MC-ICP-MS measurements (Geilert *et al.* 2015). The introduction of the quantities  $\kappa_i$  in the  $\delta$ -equation, which all have the value of unity and thus do not alter the  $\delta$ -value, but carry a specific uncertainty contribution, allows us to calculate the combined

**Table 1.**  
Instruments and operating conditions applied at the participating institutes

Parameter	BAM	GFZ	NIST	PTB	UBR
Instrument type	Neptune Plus	Neptune Plus	Neptune	Neptune	Neptune Plus
Auto sampler	Cetac ASX 100	Cetac ASX-110FR	ESI-SC-Micro	ESI-SC-Micro	Cetac ASX 112FR
Aspiration mode	Self-aspirating	Self-aspirating	Self-aspirating	Self-aspirating	Self-aspirating
Nebuliser	PFA 100 $\mu\text{l min}^{-1}$	PFA 110 $\mu\text{l min}^{-1}$	PFA 100 $\mu\text{l min}^{-1}$	PFA 150 $\mu\text{l min}^{-1}$	PFA 50 $\mu\text{l min}^{-1}$
Spray chamber	ESI cyclonic spray chamber (quartz)	Combined cyclonic & Scott (quartz)	Combined cyclonic & Scott (PEEK)	Combined cyclonic & Scott (quartz)	Combined cyclonic & Scott (quartz)
Interface	Jet	Jet	Normal	Normal	Jet
Cones	Ni sampler and Ni H skimmer	Ni sampler and Ni X skimmer	Ni sampler and Ni X skimmer	Ni sampler and Ni H skimmer	Ni sampler and Ni X skimmer
Cool gas flow rate	16 $\text{l min}^{-1}$	15 $\text{l min}^{-1}$	16 $\text{l min}^{-1}$	16 $\text{l min}^{-1}$	15 $\text{l min}^{-1}$
Auxiliary gas flow rate	0.9–1.05 $\text{l min}^{-1}$	0.7 $\text{l min}^{-1}$	$\approx 0.93 \text{ l min}^{-1}$	$\approx 0.80 \text{ l min}^{-1}$	0.80 $\text{l min}^{-1}$
Sample gas flow rate	1.00–1.15 $\text{l min}^{-1}$	1.1 $\text{l min}^{-1}$	$\approx 1.02 \text{ l min}^{-1}$	$\approx 1.05 \text{ l min}^{-1}$	$\approx 1.02 \text{ l min}^{-1}$
RF power	1200 W	1200 W	1200 W	1200 W	1170 W
Guard electrode	On	On	On	On	On
Mass resolution mode	Low	Medium	Medium	Low	Low
Faraday detectors	L3, C, H3	L2, C, H2	L3, C, H3	L3, C, H3	L3, C, H3
Gain calibration	Before each sequence	Before each sequence	Before each sequence	Before each sequence	weekly
Baseline measurement	Before each sequence	Before each sequence	Before each sequence	Before each measurement	weekly
Amplifier resistor	$10^{11} \Omega$	$10^{11} \Omega$	$10^{11} \Omega$	$10^{11} \Omega$	$10^{11} \Omega$
Integration time	4.194 s	4.194 s	4.194 s	2.097 s	8.389
Blocks/cycles	1/50	1/20	1/55	18/1	1/20
Sensitivity in $\text{V mg}^{-1} \text{ kg}^{-1}$	28 (LR) <sup>e</sup>	35 (MR) <sup>e</sup>	$\approx 8$ (MR) <sup>e</sup>	27 (LR) <sup>e</sup>	60 (LR) <sup>e</sup>
Mg mass fractions of solutions used	0.25 $\text{mg kg}^{-1}$	0.50 $\text{mg kg}^{-1}$	0.20 $\text{mg kg}^{-1}$	0.30 $\text{mg kg}^{-1}$	0.30 $\text{mg kg}^{-1}$
Typical $^{24}\text{Mg}$ blank intensity	< 2 mV	< 14 mV	$\approx 11$ mV	$\approx 5$ mV	< 10 mV
Typical isotope ratio drift <sup>b</sup>	-0.013% $\text{h}^{-1}$	0.01% $\text{h}^{-1}$	NA	-0.018% $\text{h}^{-1}$	-0.005 to 0.005% $\text{h}^{-1}$
Typical isotope ratios repeatability ( $s_{\text{rel}}$ ) <sup>c</sup>	0.008%	0.01% (s); 0.003% ( $s_m$ )	$\approx 0.02\%$	0.024%, $n = 18$	0.003%
Isotope ratio repeatability ( $s_{\text{rel}}, n$ ) <sup>d</sup>	< 0.006%, $n = 5$	< 0.005%, $n = 10$	$\approx 0.02\%$ , $n = 19$	0.0089%, $n = 25$	$\approx 0.002\%$ , $n = 32$

<sup>a</sup> Sum of all Mg ion intensities per 1  $\text{mg kg}^{-1}$  Mg in the solution.

<sup>b</sup> Drift for the  $^{26}\text{Mg}/^{24}\text{Mg}$  ratio expressed in %  $\text{h}^{-1}$ .

<sup>c</sup> Relative standard deviation  $s_{\text{rel}}$  within one measurement ( $^{26}\text{Mg}/^{24}\text{Mg}$ , ERM-AE143).

<sup>d</sup> Relative standard deviation  $s_{\text{rel}}$  of  $n$  repeated measurements ( $^{26}\text{Mg}/^{24}\text{Mg}$ , ERM-AE143).

<sup>e</sup> Mass resolution mode using a variable entrance slit, LR = low mass resolution mode, MR = medium mass resolution mode.

measurement uncertainty (obtained by combination of individual uncertainty contributions) of the  $\delta$ -value. In this study, only pure magnesium solutions were measured and therefore contributions from sample digestion and matrix separation do not need to be considered. Remaining influencing quantities are as follows:

- (1) The repeatability of the sample isotope ratio measurement
- (2) The repeatability of the preceding and following standard isotope ratio measurement
- (3) The uncertainty contribution from the nitric acid blank ( $\kappa_1$ )
- (4) The uncertainty contribution from potential standard inhomogeneity ( $\kappa_2$ )
- (5) The uncertainty contribution from fluctuation or drift of the instrumental mass bias ( $\kappa_3$ ).

Introducing the above-described modifications in Equation (1) leads to Equation (4):

$$\delta^{i/24}\text{Mg} = \delta^{i/24}\text{Mg}_{\text{ERM-AE143}} = \left( \frac{R_{\text{smp}}^{\text{meas}} \left( \frac{i}{24}\text{Mg} \right) \times \kappa_1}{R_{\text{ERM-AE143}}^{\text{meas}} \left( \frac{i}{24}\text{Mg} \right) \times \kappa_2} \times \kappa_3 \right) - 1 \quad (4)$$

where  $i = 25, 26$ .

According to international guidelines, the experimental standard deviation of the mean ( $s_m = s/\sqrt{N}$ , where  $s$  is the standard deviation) is used to express the uncertainty contribution derived from the repeatability of the isotope ratio measurements (JCGM 2008) with  $N$  repeat measurements. Based on Equation (4), the measurement uncertainty can be calculated by using specific software such as GUM



Workbench (Metrodata 2019) or by applying a simplified approach for the uncertainty propagation via the square sum of all contributions. The latter can be easily carried out in Excel or other spreadsheet software and is explained in the following for a representative sequence within which the  $\delta^{26/24}\text{Mg}$  values were determined in pure Mg solutions without any sample decomposition and matrix separation:

- (1) All contributions are expressed in absolute uncertainty contributions to the  $\delta^{26/24}\text{Mg}$  value, expressed in ‰.
- (2) The relative  $s_m$  of the measured isotope ratio,  $^{26}\text{Mg}/^{24}\text{Mg}$ , in the sample is given in ‰ and represents  $u(R_{\text{sm}})$ , for example, 0.012‰.
- (3) The relative  $s_m$  of the measured isotope ratio,  $^{26}\text{Mg}/^{24}\text{Mg}$ , in the preceding standard given in ‰ represents  $u(R_{\text{std1}})$ , for example, 0.012‰.
- (4) The relative  $s_m$  of the measured isotope ratio,  $^{26}\text{Mg}/^{24}\text{Mg}$ , in the subsequent standard given in ‰ represents  $u(R_{\text{std2}})$ , for example, 0.014‰.
- (5)  $\kappa_1$  (blank contribution) is represented by the  $s_m$  of the  $^{26}\text{Mg}$  intensity of all blank measurements in the corresponding measurement sequence, divided by the mean  $^{26}\text{Mg}$  intensity in the samples/standards and given in ‰; for example, fifty-three blank measurements gave a mean value of 0.233 mV and a standard deviation ( $s$ ) of 0.045 mV for the  $^{26}\text{Mg}$  intensity, while the mean  $^{26}\text{Mg}$  intensity in a standard is 800 mV; this results in an uncertainty contribution of the blank of  $\approx 0.0077\%$ .
- (6)  $\kappa_2$  (standard inhomogeneity) is obtained from the certification report of the standard, ERM-AE143; it is represented by the potential between-bottle-inhomogeneity  $u_{\text{bb}}$  given in ‰; for example,  $u_{\text{bb}} \approx 0.010\%$ .
- (7)  $\kappa_3$  (mass bias drift) is obtained from the overall drift of the bracketing standard within one sequence (last standard isotope ratio minus first standard isotope ratio, divided by first standard isotope ratio) given in ‰ and divided by the number of sample measurements times two; for example, overall drift for  $\delta^{26/24}\text{Mg}$  in the sequence with  $N = 24$  sample measurements is 0.554‰; thus, the uncertainty contribution due to mass bias drift is 0.012‰.
- (8) All contributions are combined in Equation (5).

$$u\left(\delta^{26/24}\text{Mg}_{\text{ERM-AE143}}\right) = \sqrt{u^2(R_{\text{sm}}) + u^2(R_{\text{std1}}) + u^2(R_{\text{std2}}) + u^2(\kappa_1) + u^2(\kappa_2) + u^2(\kappa_3)} \quad (5)$$

With the example values given above, we obtain a combined standard uncertainty  $u_c$  for the  $\delta^{26/24}\text{Mg}$  value of

0.028‰ and an expanded uncertainty  $U$  ( $k = 2$ , represents 95% confidence) of 0.056‰. The combined measurement uncertainty was calculated for each individual  $\delta$ -value. Then, all obtained  $\delta$ -values for each specific sample were averaged; the combined standard uncertainties were averaged according to Equation (6) and combined with the spread of the results according to Equation (7). The outcome of these calculations is then used as the combined uncertainty, or, after multiplication by two ( $k = 2$ , representing 95% confidence level), as the expanded uncertainty  $U$  for the final  $\delta$ -value.

$$\bar{u} = \sqrt{\frac{\sum_i u_i^2}{N}} \quad (6)$$

$$u_c = \sqrt{\left(\frac{s}{\sqrt{N}}\right)^2 + \bar{u}^2} \quad (7)$$

The final  $\delta$ -values and their associated measurement uncertainties are compiled in Tables S1 and S2 of the supplementary material.

**Analytical procedure applied at GFZ:** Magnesium isotope ratios were determined at the Helmholtz Laboratory for the Geochemistry of the Earth Surface (HELGES) at GFZ Potsdam. Prior to Mg isotope analyses, all solutions were evaporated in PFA vials on a hot plate in a HEPA-filtered laminar flow workstation. Then, they were re-dissolved in the same batch of  $\text{HNO}_3$  (0.3 mol l<sup>-1</sup>) and diluted to a Mg mass fraction of 0.50 mg kg<sup>-1</sup> to ascertain acid molarity and Mg mass fraction matching between all solutions used for isotope ratio measurements. In addition, one measurement of each solution was also performed by direct dilution from the stock bottles with  $\text{HNO}_3$  of 0.3 mol l<sup>-1</sup>. Mg isotope ratios were determined using a MC-ICP-MS under operating conditions as described in Table 1. In order to ensure interference-free measurements, all Mg isotope signals ( $^{24}\text{Mg}^+$ ,  $^{25}\text{Mg}^+$ ,  $^{26}\text{Mg}^+$ ) were measured in medium mass resolution mode;  $^{26}\text{Mg}^+$  was measured on the interference-free low mass side of the flat-top peak (to avoid potential interference from  $^{12}\text{C}^{14}\text{N}^+$ ). Signal intensities of  $^{23}\text{Na}^+$  and  $^{27}\text{Al}^+$  were simultaneously monitored (in Faraday cups L4 and H4) for each measurement to verify the purity of the analyte solutions (purity was always  $> 0.997$  kg kg<sup>-1</sup> Mg). All Mg solutions were measured using SSB blocks with an on-peak measured blank (0.3 mol l<sup>-1</sup>  $\text{HNO}_3$ ) before and after each block. Measurements were repeated in three different analytical sessions, each on a different day, including new sample dilutions (as described above) and instrument optimisation. Each individual  $\delta^{i/24}\text{Mg}$  analysis

comprised a full repeat of a SSB block, separated in time by several hours.

Outlier-corrected data (based on the 2s criterion) for the blank, sample and standard measurements were collected and copied into Excel for further calculations. Averaged values for the preceding and subsequent blank were subtracted from the corresponding measurement of the sample and of the standard. From the blank-corrected signal ratios,  $\delta$ -values were obtained according to Equation (1).

Typical repeatability for the  $^{26}\text{Mg}/^{24}\text{Mg}$  ratio was  $< 0.0003\%$  ( $s_m$  on  $N = 20$  integrations of 4.2 s each). The uncertainty associated with the reported Mg  $\delta$ -values was evaluated in a similar way as described for BAM (see Analytical procedure applied at BAM), following Equation (4). The standard uncertainties are expressed as  $s_m$  ( $=s/\sqrt{N}$  on  $N = 20$  integrations of 4.2 s each) in the measured isotope ratios ( $^{26}\text{Mg}/^{24}\text{Mg}$  and  $^{25}\text{Mg}/^{24}\text{Mg}$ ) of the sample ( $u(R_{\text{sample}}) < 0.003\%$  on the  $^{26}\text{Mg}/^{24}\text{Mg}$  ratio, for example), the two bracketing standards ( $u(R_{\text{std1}}) < 0.03\%$  and  $u(R_{\text{std2}}) < 0.003\%$ ), and the blank ( $u(\kappa_3) < 0.03\%$  on the  $^{26}\text{Mg}/^{24}\text{Mg}$  ratio, for example). Then, we obtain a combined standard uncertainty  $u_c$  for the  $\delta^{26/24}\text{Mg}$  value of  $0.047\%$  and an expanded uncertainty  $U$  ( $k = 2$ ) of  $0.094\%$  for example. We note that the uncertainty contribution of the blank-correction  $u(\kappa_3)$  is most likely overestimated in this calculation, because the signal intensity of the blank relative to the sample or bracketing standard intensity is  $< 0.04\%$ , and a change in the  $\delta^{26/24}\text{Mg}$  value caused by the blank correction of  $< 0.01\%$  was observed.

The combined measurement uncertainty for each measured  $\delta$ -value (individual SSB blocks) was calculated for each individual  $\delta$ -value. Then, all  $\delta$ -values for each specific sample obtained by repeat analysis were averaged and reported in Tables S1 and S2. The associated individual combined standard uncertainties were also averaged ( $u_c$  in Tables S1 and S2), and the expanded uncertainty values ( $U$ , Tables S1 and S2) were calculated by multiplication of  $u_c$  with  $k = 2$ , yielding typically  $U(\delta^{26/24}\text{Mg}) < 0.12\%$  and  $U(\delta^{25/24}\text{Mg}) < 0.074\%$ , respectively. The  $s$  of repeat SSB measurements (Tables S1 and S2) is typically  $< 0.054\%$  for  $\delta^{26/24}\text{Mg}$  and  $< 0.033\%$  for  $\delta^{25/24}\text{Mg}$ , respectively, which is consistent with long-term observations based on repeat measurements of Cambridge1 ( $N > 125$ ) and different matrix reference materials (measured after Mg column purification) over the course of  $> 3$  years at GFZ (Pokharel *et al.* 2017, 2018, Uhlig *et al.* 2017, Shalev *et al.* 2018, Schuessler *et al.* 2018),

estimated to be  $\pm 0.027\%$  ( $s$ ) for  $\delta^{25/24}\text{Mg}$  and  $\pm 0.047\%$  ( $s$ ) for  $\delta^{26/24}\text{Mg}$ , respectively.

In every measurement session, the Mg  $\delta$ -values of the artefact standard Cambridge1 (pure Mg solution) were determined repeatedly to assess precision and accuracy and showed good agreement with compiled data for Cambridge1 from the literature (e.g., compilations in Foster *et al.* 2010, Pogge von Strandmann *et al.* 2011, Ling *et al.* 2011, An and Huang 2014, Teng 2017, and references therein).

**Analytical procedure applied at NIST:** All provided samples were diluted to a Mg mass fraction of  $0.20 \text{ mg kg}^{-1}$  with dilute  $\text{HNO}_3$  ( $20 \text{ g kg}^{-1}$ ). All measurements were made on a Thermo Scientific Neptune MC-ICP-MS under operating conditions as specified in Table 1. Normal SSB procedure was applied using ERM-AE143 as the bracketing standard.

All the supplied samples were measured in three completely independent sequences over days. Note that the NIST SRM 980 and IRMM-009 measurements apply only to the solutions supplied to NIST by BAM. For each sequence, three  $\delta^{26/24}\text{Mg}$  values of each material were determined and the measurements for the three  $\delta^{26/24}\text{Mg}$  values were spaced evenly over the early, middle and late portions of the run sequence. A total of nine  $\delta^{26/24}\text{Mg}$  determinations of each material were made, taken over the three independent sequences.

Measurements were made at medium mass resolution. The static multi-collection set-up was optimised such that the low mass edges of the  $^{24}\text{Mg}$  (L3),  $^{25}\text{Mg}$  (C) and  $^{26}\text{Mg}$  (H3) were aligned on their low mass sides. The point of measurement was then shifted approximately 11 milli-mass units to the low mass side of the centroid of the  $^{25}\text{Mg}$  peak (centre Faraday cup) to avoid any possibilities of hydride interferences. As the analytical performance is comparable to that of PTB (see below), the median of the measurement uncertainties reported by PTB for the  $\delta^{26/24}\text{Mg}$  values, which is  $0.062\%$ , was used for the NIST data. The final  $\delta$ -values and their associated measurement uncertainties are compiled in Tables S1 and S2.

**Analytical procedure applied at PTB:** A similar set-up and experimental conditions (as described in Vogl *et al.* 2016) for isotope amount ratio measurements were used; instrumental parameters are listed in Table 1. Within this project, however,  $\delta$ -measurements were required and no absolute isotope ratio measurements. Therefore, some modifications were necessary. The Mg mass fraction in the

solutions measured was reduced from 1.50 to 0.30 mg kg<sup>-1</sup>. Consequently, the typical repeatability of an MC-ICP-MS measurement calculated from eighteen individual measurements increased from < 0.002% (Vogl *et al.* 2016) to approximately 0.024% in this study. To run the isotope  $\delta$ -measurements, a SSB approach was applied, with a blank measurement before each standard and before each sample. All iRM and artefact standards were measured four times within each sequence in a highly symmetric order to cancel any uncorrected drift contribution. Four measurement sequences were performed on different days, one of which was discarded due to unacceptable high uncertainties of unknown origin. The typical drift of the <sup>26</sup>Mg/<sup>24</sup>Mg ratio was 0.018% h<sup>-1</sup> calculated from the measurements of ERM-AE143 during the sequences.

No outlier correction was applied. Each sample was measured with eighteen blocks and one cycle/block. After each block, the amplifier/resistor cup connection was switched ('rotating amplifiers') to avoid any influence of an imperfect gain calibration, although it is assumed that gain calibration effects largely cancel in  $\delta$ -measurements. Prior to each measurement, the ion beam was defocussed, and the electronic baseline of every Faraday cup used was acquired for 30 s and automatically subtracted from the recorded signals.

No further treatment of the raw data was carried out using the Thermo Scientific Neptune software. The raw data were then exported to Excel. Every single measurement of a certain sequence is defined by a unique index increasing with time  $t$ . Sections consisting of seven measurements were evaluated to yield a single  $\delta$ -value. The sequence within each section is blank ( $i - 3$ ), 1st reference ( $i - 2$ ), blank ( $i - 1$ ), sample ( $i$ ), blank ( $i + 1$ ), 2nd reference ( $i + 2$ ) and blank ( $i + 3$ ), with the (time) indices given in brackets. The blank intensities  $I_{bl}(iMg)$  acquired before and after the reference and the sample were averaged and subtracted from the corresponding averaged individual signal intensities  $I_{AE143}(iMg)$  and  $I_x(iMg)$ , respectively:

$$I_{AE143}^{i-2,corr}(iMg) = I_{AE143}^{i-2}(iMg) - \frac{I_{bl}^{i-3}(iMg) + I_{bl}^{i-1}(iMg)}{2}$$

$$I_x^{i,corr}(iMg) = I_x^i(iMg) - \frac{I_{bl}^{i-1}(iMg) + I_{bl}^{i+1}(iMg)}{2}$$

$$I_{AE143}^{i+2,corr}(iMg) = I_{AE143}^{i+2}(iMg) - \frac{I_{bl}^{i+1}(iMg) + I_{bl}^{i+3}(iMg)}{2}$$

These blank-corrected intensities were then combined to calculate the resulting four  $\delta$ -values per sequence:

$$\begin{aligned} \delta^{i/24}Mg_i &= \delta^{i/24}Mg_{ERM-AE143,i} \\ &= \left( \frac{I_x^{i,corr}(iMg)}{I_x^{i,corr}(24Mg)} \right) - 1 \quad (8) \\ &= \left( \frac{1}{2} \times \left( \frac{I_{AE143}^{i-2,corr}(iMg)}{I_{AE143}^{i-2,corr}(24Mg)} + \frac{I_{AE143}^{i+2,corr}(iMg)}{I_{AE143}^{i+2,corr}(24Mg)} \right) \right) - 1 \end{aligned}$$

Using the above-described method, the three sequences yielded twelve  $\delta$ -values per sample. The final  $\delta$ -value was calculated as their arithmetic mean.

For a comprehensive discussion of potential sources of biases, refer to section *Analytical procedure applied at BAM*. To minimise any bias introduced by different compositions of sample and standard, all samples and standards were diluted using the same nitric acid stock solution and all samples and standards were 'concentration'-matched to within  $\pm 10\%$  following a preceding screening of the Mg mass fractions using the MC-ICP-MS.

The uncertainties associated with the  $\delta$ -values were calculated according to the 'Guide to the Expression of Uncertainty in Measurement' (GUM) (JCGM 2008) using the software GUM Workbench Pro 2.4.1 (Metrodata 2019). Equation (8) served as the model equation. The best estimates for the input quantities were calculated as the arithmetic means of the twelve intensity ratios (three sequences with four values each) in case of the samples and of the twenty-four ratios (three sequences with eight values each) in case of the reference. Their associated uncertainties were estimated as the type A standard uncertainty within each sequence contributing four values in case of the samples and eight in case of the reference. The resulting standard uncertainties were then averaged across the three sequences. In parallel, the covariances and correlation coefficients for the sample and corresponding reference intensity ratios within each sequence were calculated according to equations (17) and (14) from JCGM (2008). The correlation coefficients were also averaged across the sequences. In almost all cases, they were larger than 0.99 reflecting the reason for the evaluation of data triples (samples measurements bracketed by two reference measurements) in order to avoid any influence from a drifting mass bias. The standard uncertainties and correlation coefficients were fed into the GUM Workbench software. The variation of the  $\delta$ -values between the three sequences was added by calculating their associated type A standard uncertainty across the sequences. The final  $\delta$ -values and their associated measurement uncertainties are compiled in Tables S1 and S2.

**Analytical procedure applied at UBR:** Isotope analyses were carried out on a Thermo Scientific Neptune Plus MC-ICP-MS in the Isotope Geochemistry Laboratory at Marum –



Center for Marine Environmental Sciences, University of Bremen, Germany. The instrument was equipped with a normal interface and interface pump. All instrumental details are given in Table 1. All intercomparison samples were diluted with  $20 \text{ g kg}^{-1} \text{ HNO}_3$  to yield  $0.3 \text{ mg kg}^{-1} \text{ Mg}$  solutions ( $\pm 5\%$ ) and measured in randomly selected order using ERM-AE143 as the bracketing standard. Measurements were performed in full bracketing mode in three differently ordered, systematically organised analytical sequences on different days within two weeks using operating conditions given in Table 1. Each sample solution was analysed four times within one analytical sequence of  $\approx 17 \text{ h}$ . The sample preparation and instrument optimisation were performed separately for each sequence. A full bracketing contains measurements of two separate bracketing standards (ERM-AE143) and one sample in between.  $\text{HNO}_3$  ( $20 \text{ g kg}^{-1}$ ) was measured directly before and after each sample or standard to monitor the analytical baseline. Consequently, one complete bracketing consists of seven measurements. All raw data were copied into an Excel workbook for further offline correction and evaluation. The averaged intensities of the two blank measurements, which were measured directly before and after each sample or standard, represent the analytical baselines and were used for correction of the averaged intensities of the corresponding sample or standard. On the basis of blank-corrected intensities of samples and standards, isotope ratios were calculated followed by the  $\delta$ -values. Since all materials were provided as pure Mg solutions and measured in equal concentrations using the same batch of  $20 \text{ g kg}^{-1} \text{ HNO}_3$  as solvent, potentially formed minor abundant hydride ions remain below the detection limit (Vogl *et al.* 2016) and possible interferences like  $\text{CC}^+$ ,  $^{12}\text{C}^{14}\text{N}^+$ ,  $^{23}\text{Na}^1\text{H}^+$ , and  $^{24}\text{Mg}^1\text{H}^+$  species did not affect the  $\delta$ -values. In total, twelve  $\delta$ -values for each material were obtained and averaged. The  $\delta^{26/24}\text{Mg}_{\text{DSM3}}$  value of Cambridge1 yields  $-2.60 \pm 0.03$ , (2s)‰, which compares well to the value of  $-2.58 \pm 0.14$ , (2s)‰ reported by Galy *et al.* (2003) and demonstrates the accuracy and precision of the analytical procedure. The analytical performance of UBR is similar to that of BAM. Therefore, the median of the combined measurement uncertainties reported by BAM for the  $\delta^{25/24}\text{Mg}$ - and  $\delta^{26/24}\text{Mg}$ -values, which are 0.025‰ and 0.030‰, respectively, were chosen as combined measurement uncertainties for the UBR values. The final  $\delta$ -values and their associated measurement uncertainties are compiled in Tables S1 and S2.

## Results and discussion

### Individual units of DSM3 and Cambridge1

DSM3 and Cambridge1 are highly accepted and widely distributed artefact standards in the Mg isotope

community. As mentioned earlier, both materials do not fulfil the requirements of reference materials according to ISO 17034 (ISO 2016); nonetheless, DSM3 is the currently accepted  $\delta$ -scale for magnesium with its anchor point DSM3 as recognised by IUPAC (Brandt *et al.* 2014). DSM3 and Cambridge1 are bottled on demand without documented homogeneity checks and often aliquots are not directly coming from the original source, but were manipulated (divided, diluted etc.) and further distributed by other users. Furthermore, these materials are not commercially available, but were distributed via personal contacts for free. Therefore, it is important to check the potential variability of individual units obtained via different routes. As explained above, the authors got DSM3 via three different routes, one of which was directly provided by the producer of the solution (Galy *et al.* 2003), while Cambridge1 was obtained from two different sources. All laboratories participating in this study received DSM3 and Cambridge1 from source 'T', while two laboratories also received the materials from source 'P'; BAM additionally received the original DSM3 solution from source 'I' (see section Isotope reference materials and artefact standards for further details on the sources). The reported results for the  $\delta^{26/24}\text{Mg}_{\text{ERM-AE143}}$  values of both materials are displayed in Figure 1, with different colour codes for the individual sources. For Cambridge1 (Figure 1a), all measured  $\delta^{26/24}\text{Mg}_{\text{ERM-AE143}}$  values range between 0.624‰ and 0.741‰ and overlap with each other within the stated standard uncertainties ( $k = 1$ ). In the case of DSM3 (Figure 1b), the reported  $\delta^{26/24}\text{Mg}_{\text{ERM-AE143}}$  values range between 3.252‰ and 3.329‰ and nearly all results overlap already at the standard uncertainty standard ( $k = 1$ ) level; within their expanded uncertainties ( $k = 2$ ), all results overlap with each other.

Based on the associated expanded uncertainty, all  $\delta^{26/24}\text{Mg}_{\text{ERM-AE143}}$  values for the two Cambridge1 units are metrologically compatible with each other and cannot be distinguished from one another. The same applies for the three DSM3 units. An isotopic difference in the two Cambridge1 solutions or in the three DSM3 solutions could not be observed. The performed measurements of different batches of Cambridge1 and DSM3 are the first independent evidence for the isotopic homogeneity of both materials and points to a fit-for-purpose distribution procedure leading to unbiased artefact standards. However, due to contamination issues, a distribution of dilute batches ( $\ll 100 \text{ mg kg}^{-1}$ ) is not recommended.

### Results of the comparison and reference values

The  $\delta^{25/24}\text{Mg}_{\text{ERM-AE143}}$  values of the individual institutes obtained for the individual iRMs and artefact standards

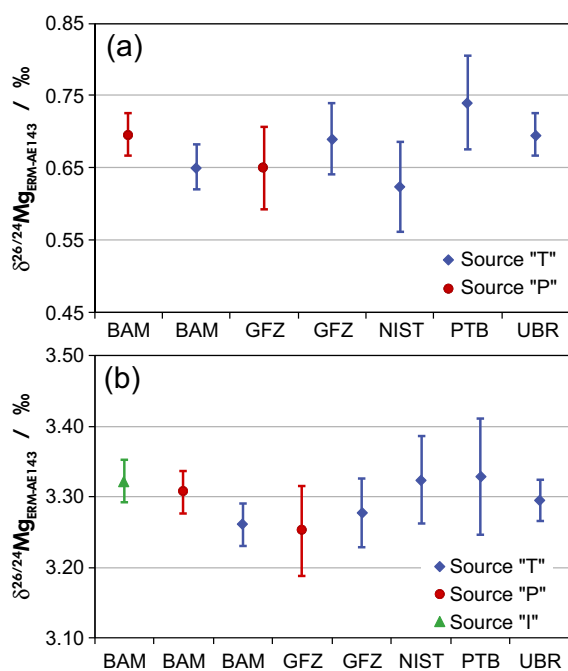


**Figure 1.**  $\delta^{26/24}\text{Mg}_{\text{ERM-AE143}}$  values for individual sources of Cambridge1 (a) and DSM3 (b) as reported by the participants; range bars depict the combined standard uncertainty.

(Figure 2, Tables S1 and S2) depict a narrow distribution with standard deviations of  $< 0.02\%$  (1s). All reported  $\delta^{25/24}\text{Mg}_{\text{ERM-AE143}}$  values agree with each other already within the reported standard uncertainties. The criterion for metrological compatibility, which commonly requires the difference of any two values to be equal to or smaller than the expanded uncertainty of said difference, hence is fulfilled. The  $\delta^{26/24}\text{Mg}_{\text{ERM-AE143}}$  values of the individual institutes obtained for the individual iRMs and artefact standards (Figure 2, Tables S1 and S2) show a slightly wider distribution compared with the  $\delta^{25/24}\text{Mg}_{\text{ERM-AE143}}$  values with standard deviations of  $< 0.05\%$ . This, however, is mainly due to the larger difference of the two isotope masses and correlates to the larger instrumental isotopic fractionation. As the reported  $\delta^{26/24}\text{Mg}_{\text{ERM-AE143}}$  values agree with each other within the reported standard uncertainties, metrological compatibility is realised as well.

Measurement uncertainties of the reported laboratory mean isotope delta values are relatively homogenous and differ not more than by a factor of 3, which mirrors the metrological quality of all results. Additionally, all results are metrologically compatible as stated above. Thus, all stated measurement uncertainties are reliable and reasonable, demonstrating that each laboratory had all sources of error

under control and came up with a realistic uncertainty calculation. Based on these findings, the uncertainty-weighted mean was chosen as the estimator for the individual reference values. The uncertainty-weighted mean  $\bar{x}_{\text{Uwm}}$  was calculated according to Equation (9) (CCQM 2013) from the results  $x_i$  provided by  $N$  laboratories:

$$\bar{x}_{\text{Uwm}} = \sum_{i=1}^N \left( \frac{\frac{x_i}{u^2(x_i)}}{\sum_{j=1}^N \left( \frac{1}{u^2(x_j)} \right)} \right) \quad (9)$$

To calculate the uncertainty  $u(\bar{x}_{\text{Uwm}})$  associated with the uncertainty-weighted mean first the consistency of the data set needs to be assessed by determining the so-called observed dispersion  $\chi_{\text{obs}}$  according to Equation (10) (CCQM 2013):

$$\chi_{\text{obs}}^2 = \sum_{i=1}^N \frac{(x_i - \bar{x}_{\text{Uwm}})^2}{u^2(x_i)} \quad (10)$$

In case the 95 percentile of  $\chi^2$  with  $N-1$  degrees of freedom  $\chi_{0.05, N-1}^2$  is larger than  $\chi_{\text{obs}}^2$  – meaning  $\chi_{0.05, N-1}^2 / \chi_{\text{obs}}^2 > 1$  – the data set is considered mutually consistent. Tables 2 and 3 summarise the results of the consistency tests. All data sets are mutually consistent. Therefore, the uncertainty  $u(\bar{x}_{\text{Uwm}})$  associated with the uncertainty-weighted mean was calculated according to Equation (11) (CCQM 2013):

$$u(\bar{x}_{\text{Uwm}}) = \sqrt{\left( \sum_{i=1}^N \frac{1}{u^2(x_i)} \right)^{-1}} \quad (11)$$

The so calculated  $\delta^{25/24}\text{Mg}_{\text{ERM-AE143}}$  and  $\delta^{26/24}\text{Mg}_{\text{ERM-AE143}}$  values and their associated uncertainties represent the assigned reference values for each iRM and artefact standard relative to ERM-AE143 (Tables 2 and 3). Please note, that ERM-AE143 was used as the bracketing standard to enable and realise the most direct traceability to the SI. The obtained reference values and their associated uncertainties were converted to the DSM3 scale, that is,  $\delta^{25/24}\text{Mg}_{\text{DSM3}}$  and  $\delta^{26/24}\text{Mg}_{\text{DSM3}}$  values by applying Equations (2, 3) (Tables 2 and 3). The conversion to the DSM3 scale, widely used in the literature, was performed to increase the usability of this comparison exercise. The presented two  $\delta$ -scale data sets (DSM3, ERM-AE143) enable the conversion of  $\delta$ -scales into one another, provided one of the intercomparison samples used here is involved. Moreover, as ERM-AE143 was used here as primary calibrator, traceability to the SI can be achieved via

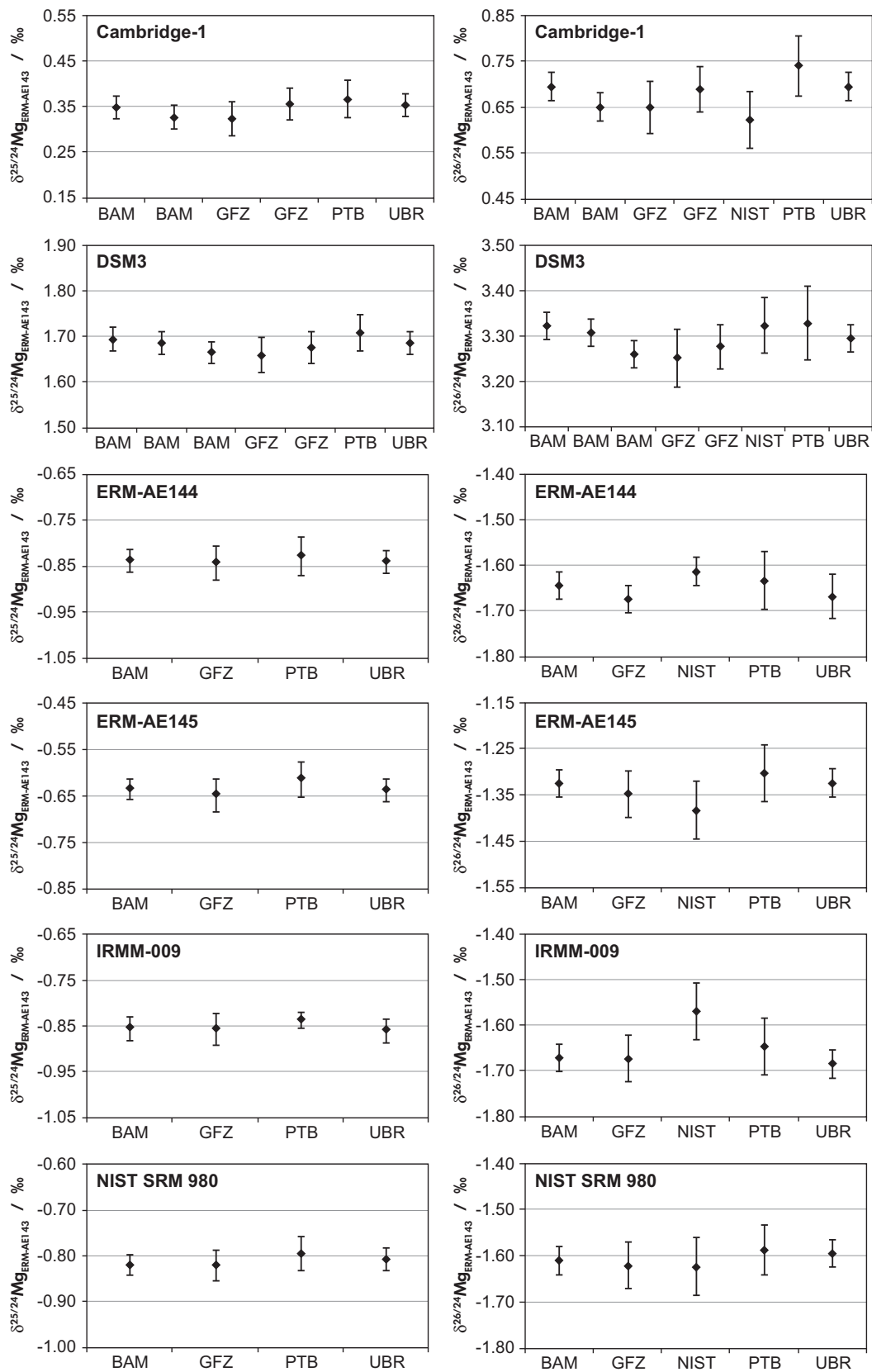


**Figure 2.**  $\delta^{25/24}\text{Mg}_{\text{ERM-AE143}}$  (left row) and  $\delta^{26/24}\text{Mg}_{\text{ERM-AE143}}$  (right row) values for all standards and iRMs investigated as reported by the participants; range bars depict the combined standard uncertainty.

**Table 2.**

Assigned reference values of the individual standards and reference materials displayed as  $\delta^{25/24}\text{Mg}_{\text{ERM-AE143}}$  values and  $\delta^{25/24}\text{Mg}_{\text{DSM3}}$  values with their associated expanded uncertainty

Standard/ iRM	$\delta^{25/24}\text{Mg}_{\text{ERM-AE143}}$ (‰)	$\frac{\chi_{0.05,N-1}^2}{\chi_{\text{obs}}^2}$	$u_c$ (‰)	$U$ (‰)	$\delta^{25/24}\text{Mg}_{\text{DSM3}}$ (‰)	$u_c$ (‰)	$U$ (‰)
Cambridge1	0.346	7.7	0.012	0.024	-1.335	0.016	0.032
DSM3	1.684	7.9	0.011	0.022	0.000	0.015	0.030
ERM-AE143	0.000		0.000	0.000	-1.681	0.011	0.021
ERM-AE144	-0.838	93	0.015	0.029	-2.517	0.018	0.036
ERM-AE145	-0.634	17	0.014	0.028	-2.313	0.018	0.036
IRMM-009	-0.848	11	0.011	0.023	-2.528	0.016	0.031
NIST SRM 980	-0.812	18	0.014	0.028	-2.491	0.018	0.035

$\delta^{25/24}\text{Mg}_{\text{ERM-AE143}}$  values were achieved as uncertainty-weighted means of the reported results;  $\delta^{25/24}\text{Mg}_{\text{DSM3}}$  values were obtained by converting the  $\delta^{25/24}\text{Mg}_{\text{ERM-AE143}}$  values to the DSM3 scale. The measured data sets were checked for mutual consistency. They are considered consistent in case  $\chi_{0.05,N-1}^2/\chi_{\text{obs}}^2 > 1$ .

**Table 3.**

Assigned reference values of the individual standards and reference materials displayed as  $\delta^{26/24}\text{Mg}_{\text{ERM-AE143}}$  values and  $\delta^{26/24}\text{Mg}_{\text{DSM3}}$  values with their associated expanded uncertainty

Standard/ iRM	$\delta^{26/24}\text{Mg}_{\text{ERM-AE143}}$ (‰)	$\frac{\chi_{0.05,N-1}^2}{\chi_{\text{obs}}^2}$	$u_c$ (‰)	$U$ (‰)	$\delta^{26/24}\text{Mg}_{\text{DSM3}}$ (‰)	$u_c$ (‰)	$U$ (‰)
Cambridge1	0.680	3.6	0.015	0.030	-2.606	0.020	0.040
DSM3	3.295	4.5	0.013	0.027	0.000	0.019	0.038
ERM-AE143	0.000		0.000	0.000	-3.284	0.013	0.027
ERM-AE144	-1.652	9.9	0.018	0.035	-4.930	0.022	0.044
ERM-AE145	-1.329	8.5	0.018	0.036	-4.609	0.022	0.045
IRMM-009	-1.656	2.6	0.014	0.029	-4.934	0.020	0.039
NIST SRM 980	-1.605	27	0.018	0.035	-4.884	0.022	0.044

$\delta^{26/24}\text{Mg}_{\text{ERM-AE143}}$  values were achieved as uncertainty-weighted means of the reported results;  $\delta^{26/24}\text{Mg}_{\text{DSM3}}$  values were obtained by converting the  $\delta^{26/24}\text{Mg}_{\text{ERM-AE143}}$  values to the DSM3 scale. The measured data sets were checked for mutual consistency. They are considered consistent in case  $\chi_{0.05,N-1}^2/\chi_{\text{obs}}^2 > 1$ .

each of the intercomparison samples provided the associated uncertainties are propagated. Although ERM-AE143 is an iRM certified for Mg isotope amount ratios and thus would perfectly be suited as a  $\delta = 0$  standard for the Mg  $\delta$ -scale, we recommend maintaining the current DSM3 scale. To enable SI traceability and scale continuity, the DSM3 scale is from now on anchored by ERM-AE143 at -1.681‰ for  $\delta^{25/24}\text{Mg}_{\text{DSM3}}$  and -3.284‰ for  $\delta^{26/24}\text{Mg}_{\text{DSM3}}$ , respectively. Of course, the artefact standard DSM3 will keep its value ( $\delta = 0$ ‰) due to the definition of the scale, but it will be attributed with a minute expanded uncertainty ( $k = 2$ ) of 0.031‰ and 0.037‰, respectively, for the  $\delta^{25/24}\text{Mg}_{\text{DSM3}}$  and the  $\delta^{26/24}\text{Mg}_{\text{DSM3}}$ . Thus, the  $\delta$ -values for DSM3 now read  $(0.000 \pm 0.031)\text{‰}$  for  $\delta^{25/24}\text{Mg}_{\text{DSM3}}$  and  $(0.000 \pm 0.037)\text{‰}$  for  $\delta^{26/24}\text{Mg}_{\text{DSM3}}$ . This offset anchoring is necessary, because first DSM3 is no reference material certified for isotope amount ratios, with all associated disadvantages, and second the DSM3 scale should be maintained for (inter)comparability of research results.

The excellent intercalibration between all  $\delta$ -scales is being confirmed by the perfect agreement of the  $\delta^{25/24}\text{Mg}_{\text{DSM3}}$  value of  $(-1.335 \pm 0.032)\text{‰}$  for Cambridge1 obtained here with the  $\delta^{25/24}\text{Mg}_{\text{DSM3}}$  value of  $(-1.342 \pm 0.040)\text{‰}$  obtained as arithmetic mean from the GeoReM database (GeoReM 2019); the  $\delta^{26/24}\text{Mg}_{\text{DSM3}}$  value of  $(-2.606 \pm 0.040)\text{‰}$  for Cambridge1 obtained agrees excellent as well with the  $\delta^{26/24}\text{Mg}_{\text{DSM3}}$  value of  $(-2.610 \pm 0.069)\text{‰}$  obtained as arithmetic mean from the GeoReM database (GeoReM 2019). Note, the  $\delta$ -values obtained in this study are accompanied by an expanded uncertainty ( $k = 2$ ); the mean values from GeoReM are accompanied by the twofold standard deviation (2s).

### Absolute Mg isotope composition of iRMs and artefact standards

An SI-traceable scale anchor, which is certified for isotope amount ratios, enables the user to calculate isotope

amount ratios  $R_i$ , isotope amount fractions  $x_i$  and molar masses (numerically equal to atomic weights  $A_i$ ) from  $\delta$ -values for any sample measured within this scale. The course of calculations is given by Equations (12–14) for the example of Mg:

$$R_{\text{smpl}}^{\text{true}} \left( \frac{i\text{Mg}}{24\text{Mg}} \right) = \left( \delta_{24}^i \text{Mg}_{\text{ERM-AE143}} + 1 \right) \times R_{\text{ERM-AE143}}^{\text{cert}} \left( \frac{i\text{Mg}}{24\text{Mg}} \right) \text{ where } i = 25, 26 \quad (12)$$

$$x_{\text{smpl}}(i\text{Mg}) = \frac{\left( \delta_{24}^i \text{Mg}_{\text{ERM-AE143}} + 1 \right) \times R_{\text{ERM-AE143}}^{\text{cert}} \left( \frac{i\text{Mg}}{24\text{Mg}} \right)}{1 + \left( \delta_{24}^{25} \text{Mg}_{\text{ERM-AE143}} + 1 \right) \times R_{\text{ERM-AE143}}^{\text{cert}} \left( \frac{25\text{Mg}}{24\text{Mg}} \right) + \left( \delta_{24}^{26} \text{Mg}_{\text{ERM-AE143}} + 1 \right) \times R_{\text{ERM-AE143}}^{\text{cert}} \left( \frac{26\text{Mg}}{24\text{Mg}} \right)} \text{ where } i = 24, 25, 26 \quad (13)$$

$$M_{\text{smpl}}(\text{Mg}) = \frac{M(24\text{Mg}) + M(25\text{Mg}) \times \left( \delta_{24}^{25} \text{Mg}_{\text{ERM-AE143}} + 1 \right) \times R_{\text{ERM-AE143}}^{\text{cert}} \left( \frac{25\text{Mg}}{24\text{Mg}} \right) + M(26\text{Mg}) \times \left( \delta_{24}^{26} \text{Mg}_{\text{ERM-AE143}} + 1 \right) \times R_{\text{ERM-AE143}}^{\text{cert}} \left( \frac{26\text{Mg}}{24\text{Mg}} \right)}{1 + \left( \delta_{24}^{25} \text{Mg}_{\text{ERM-AE143}} + 1 \right) \times R_{\text{ERM-AE143}}^{\text{cert}} \left( \frac{25\text{Mg}}{24\text{Mg}} \right) + \left( \delta_{24}^{26} \text{Mg}_{\text{ERM-AE143}} + 1 \right) \times R_{\text{ERM-AE143}}^{\text{cert}} \left( \frac{26\text{Mg}}{24\text{Mg}} \right)} \quad (14)$$

where  $i = 24, 25, 26$ . Applying Equations (12–14), the isotope amount ratios, isotope amount fractions and molar masses or atomic weights for all analysed iRMs and artefact standards were calculated from the assigned reference  $\delta$ -values (Tables 2 and 3) obtained on the ERM-AE143 scale and are compiled in Table 4, together with literature data from publications or certificates. To enable a quick comparison of the data, the so-called normalised error  $E_n$  value is added to Table 4. The  $E_n$  value is used for the assessment whether or not two data are metrologically compatible, in other words whether or not they agree within their stated uncertainties (ISO 2010). The mathematical background is presented in Equations (15–17). Consequentially, two values are metrologically compatible, when their associated  $E_n$  value is  $\leq 1$ .

$$d_{ij} = x_i - x_j \quad (15)$$

$$u^2(d_{ij}) = u^2(x_i) + u^2(x_j) - 2 \times \text{cov}(x_i, x_j) \quad (16)$$

$$E_n = \frac{|d_{ij}|}{U(d_{ij})} \quad (17)$$

The isotopic compositions for ERM-AE144 and ERM-AE145 obtained from the  $\delta$ -values agree perfectly well with those stated in the certificates, demonstrating the high

analytical quality of this study. The  $E_n$  values are  $\leq 0.1$  and  $0.2$ , respectively, indicating the difference between the values is less than 10% and 20% of the associated uncertainty, which in turn means that no difference at all can be observed within the limits of the measurement uncertainty. The isotopic composition of NIST SRM 980 obtained from the  $\delta$ -values agrees sufficiently well within the stated uncertainties with those from the certificates with  $E_n$  values of  $\leq 1$ , except for the isotope amount ratio  $n(25\text{Mg})/n(24\text{Mg})$ , which is 1.09. The isotopic compositions

of IRMM-009 obtained from the  $\delta$ -values agree slightly less with certificate data compared with NIST SRM 980. This points to the heterogeneity issue with the NIST SRM 980 material as discussed in the introduction. The isotopic composition of Cambridge1 and DSM3 obtained from the  $\delta$ -values does not agree at all with those calculated from the isotope amount ratios published by Bizzarro *et al.* (2011) with  $E_n$  values up to 5.9. When looking at the individual  $E_n$  values, it is obvious that the major difference is caused by the isotope amount fraction  $x(25\text{Mg})$  and the corresponding isotope amount ratio  $n(25\text{Mg})/n(24\text{Mg})$  with  $E_n$  values of 5.9 and 5.5, respectively. Bizzarro *et al.* state in their paper that 'If our assumption is not valid and the instrument mass discrimination is, in fact, best explained by a kinetic process ( $\beta = 0.511$ ), then our proposed  $25\text{Mg}/24\text{Mg}$  value may be inaccurate by  $\sim 1100$  ppm, although the  $26\text{Mg}/24\text{Mg}$  will remain unchanged'. We found that the  $n(25\text{Mg})/n(24\text{Mg})$  value for Cambridge1 and DSM3 published by Bizzarro *et al.* (2011) is high by  $\approx +0.9\%$ , which agrees with the above statement, while the  $n(26\text{Mg})/n(24\text{Mg})$  value is low by  $\approx -0.9\%$  compared with our data.

With the presented intercalibration of  $\delta$ -scales, the isotope amount ratios, isotope amount fractions and atomic weights of the currently used artefact standards



Table 4.

Isotope amount ratios, isotope amount fractions and molar masses of the investigated iRMs and artefact standards calculated from the  $\delta$ -values (vs. ERM-AE143) and those from certificates and from the literature with their associated expanded uncertainties ( $k = 2$ )

Standard/ iRM	Quantity	Unit	This work		Literature		$E_n$	Ref.
			Value	$U$	Value	$U$		
Cambridge1	Isotope amount ratio $n(^{25}\text{Mg})/n(^{24}\text{Mg})$	mol mol <sup>-1</sup>	0.126634	0.000020	0.126744	n/a	5.51	<sup>a</sup>
	Isotope amount ratio $n(^{26}\text{Mg})/n(^{24}\text{Mg})$	mol mol <sup>-1</sup>	0.139457	0.000043	0.139325	n/a	3.06	<sup>a</sup>
	Isotope amount fraction $n(^{24}\text{Mg})/n(\text{Mg})$	mol mol <sup>-1</sup>	0.789833	0.000030	0.789847	n/a	0.47	<sup>b</sup>
	Isotope amount fraction $n(^{25}\text{Mg})/n(\text{Mg})$	mol mol <sup>-1</sup>	0.100020	0.000015	0.100108	n/a	5.90	<sup>b</sup>
	Isotope amount fraction $n(^{26}\text{Mg})/n(\text{Mg})$	mol mol <sup>-1</sup>	0.110148	0.000030	0.110045	n/a	3.42	<sup>b</sup>
	Molar mass of Mg in solution $M(\text{Mg})$	g mol <sup>-1</sup>	24.305166	0.000058	24.305051	n/a	1.99	<sup>b</sup>
DSM3	Isotope amount ratio $n(^{25}\text{Mg})/n(^{24}\text{Mg})$	mol mol <sup>-1</sup>	0.126803	0.000020	0.126914	n/a	5.54	<sup>a</sup>
	Isotope amount ratio $n(^{26}\text{Mg})/n(^{24}\text{Mg})$	mol mol <sup>-1</sup>	0.139821	0.000043	0.139691	n/a	3.03	<sup>a</sup>
	Isotope amount fraction $n(^{24}\text{Mg})/n(\text{Mg})$	mol mol <sup>-1</sup>	0.789500	0.000030	0.789512	n/a	0.40	<sup>b</sup>
	Isotope amount fraction $n(^{25}\text{Mg})/n(\text{Mg})$	mol mol <sup>-1</sup>	0.100111	0.000015	0.100200	n/a	5.93	<sup>b</sup>
	Isotope amount fraction $n(^{26}\text{Mg})/n(\text{Mg})$	mol mol <sup>-1</sup>	0.110389	0.000030	0.110287	n/a	3.39	<sup>b</sup>
	Molar mass of Mg in solution $M(\text{Mg})$	g mol <sup>-1</sup>	24.305740	0.000058	24.305626	n/a	1.96	<sup>b</sup>
IRMM-009	Isotope amount ratio $n(^{25}\text{Mg})/n(^{24}\text{Mg})$	mol mol <sup>-1</sup>	0.126483	0.000020	0.12663	0.00013	1.12	<sup>c</sup>
	Isotope amount ratio $n(^{26}\text{Mg})/n(^{24}\text{Mg})$	mol mol <sup>-1</sup>	0.139131	0.000043	0.13932	0.00026	0.72	<sup>c</sup>
	Isotope amount fraction $n(^{24}\text{Mg})/n(\text{Mg})$	mol mol <sup>-1</sup>	0.790130	0.000030	0.78992	0.00018	1.15	<sup>c</sup>
	Isotope amount fraction $n(^{25}\text{Mg})/n(\text{Mg})$	mol mol <sup>-1</sup>	0.099938	0.000015	0.100028	0.000094	0.95	<sup>c</sup>
	Isotope amount fraction $n(^{26}\text{Mg})/n(\text{Mg})$	mol mol <sup>-1</sup>	0.109932	0.000030	0.11005	0.00018	0.65	<sup>c</sup>
	Molar mass of Mg in solution $M(\text{Mg})$	g mol <sup>-1</sup>	24.304653	0.000058	24.30498	0.00036	0.90	<sup>c</sup>
NIST SRM 980	Isotope amount ratio $n(^{25}\text{Mg})/n(^{24}\text{Mg})$	mol mol <sup>-1</sup>	0.126487	0.000020	0.12663	0.00013	1.09	<sup>d</sup>
	Isotope amount ratio $n(^{26}\text{Mg})/n(^{24}\text{Mg})$	mol mol <sup>-1</sup>	0.139138	0.000043	0.13932	0.00026	0.69	<sup>d</sup>
	Isotope amount fraction $n(^{24}\text{Mg})/n(\text{Mg})$	mol mol <sup>-1</sup>	0.790123	0.000030	0.78992	0.00025	0.81	<sup>d</sup>
	Isotope amount fraction $n(^{25}\text{Mg})/n(\text{Mg})$	mol mol <sup>-1</sup>	0.099941	0.000015	0.10003	0.00009	0.98	<sup>d</sup>
	Isotope amount fraction $n(^{26}\text{Mg})/n(\text{Mg})$	mol mol <sup>-1</sup>	0.109936	0.000030	0.11005	0.00019	0.59	<sup>d</sup>
	Molar mass of Mg in solution $M(\text{Mg})$	g mol <sup>-1</sup>	24.304665	0.000058	24.30497	0.00044	0.69	<sup>e</sup>
ERM-AE144	Isotope amount ratio $n(^{25}\text{Mg})/n(^{24}\text{Mg})$	mol mol <sup>-1</sup>	0.126484	0.000020	0.126486	0.000022	0.07	<sup>f</sup>
	Isotope amount ratio $n(^{26}\text{Mg})/n(^{24}\text{Mg})$	mol mol <sup>-1</sup>	0.139132	0.000043	0.139138	0.000039	0.11	<sup>f</sup>
	Isotope amount fraction $n(^{24}\text{Mg})/n(\text{Mg})$	mol mol <sup>-1</sup>	0.790129	0.000030	0.790124	0.000039	0.11	<sup>f</sup>
	Isotope amount fraction $n(^{25}\text{Mg})/n(\text{Mg})$	mol mol <sup>-1</sup>	0.099939	0.000015	0.099939	0.000013	0.02	<sup>f</sup>
	Isotope amount fraction $n(^{26}\text{Mg})/n(\text{Mg})$	mol mol <sup>-1</sup>	0.109932	0.000030	0.109936	0.000025	0.10	<sup>f</sup>
	Molar mass of Mg in solution $M(\text{Mg})$	g mol <sup>-1</sup>	24.304655	0.000058	24.304664	0.000063	0.11	<sup>f</sup>
ERM-AE145	Isotope amount ratio $n(^{25}\text{Mg})/n(^{24}\text{Mg})$	mol mol <sup>-1</sup>	0.126510	0.000020	0.126514	0.000016	0.16	<sup>g</sup>
	Isotope amount ratio $n(^{26}\text{Mg})/n(^{24}\text{Mg})$	mol mol <sup>-1</sup>	0.139177	0.000043	0.139185	0.000029	0.16	<sup>g</sup>
	Isotope amount fraction $n(^{24}\text{Mg})/n(\text{Mg})$	mol mol <sup>-1</sup>	0.790085	0.000030	0.790078	0.000028	0.17	<sup>g</sup>
	Isotope amount fraction $n(^{25}\text{Mg})/n(\text{Mg})$	mol mol <sup>-1</sup>	0.099953	0.000015	0.099956	0.000010	0.14	<sup>g</sup>
	Isotope amount fraction $n(^{26}\text{Mg})/n(\text{Mg})$	mol mol <sup>-1</sup>	0.109961	0.000030	0.109967	0.000021	0.15	<sup>g</sup>
	Molar mass of Mg in solution $M(\text{Mg})$	g mol <sup>-1</sup>	24.304728	0.000058	24.304741	0.000046	0.17	<sup>g</sup>

$E_n$  value, the so-called normalized error, depicts metrological compatibility of two values, when  $E_n \leq 1$ , calculated by using Equations 15–17.

<sup>a</sup> Data from Bizzarro *et al.* (2011); because no uncertainties were provided, the values were truncated and rounded to six digits.

<sup>b</sup> Data calculated from the isotope ratios; no uncertainties can be provided, because no uncertainties for the isotope ratios are available.

<sup>c</sup> Data from certificate of IRMM-009 (IRMM, 2018).

<sup>d</sup> Data from certificate of NIST SRM 980 (NIST 1967).

<sup>e</sup> Data from Catanzaro *et al.* (1966).

<sup>f</sup> Data from certificate of ERM-AE144 (BAM 2018b).

<sup>g</sup> Data from certificate of ERM-AE145 (BAM 2018c).

can be calculated. This calculation, however, is possible for any sample from any scale whose anchor has been calibrated against ERM-AE143 within this study. After converting the  $\delta$ -values to the ERM-AE143 scale using Equation (3), the isotope amount ratios, isotope amount fractions and atomic weights can be calculated using Equations (12–14).

### Triple isotope fractionation

**Consistency of isotope  $\delta$ -values with absolute isotope ratio determinations:** ERM-AE144 and ERM-AE145 measured against ERM-AE143 by standard-sample bracketing yield  $\delta$ -values in agreement with  $\delta$ -values calculated from absolute isotope ratios from Vogl *et al.* (2016) (Figure 3a).

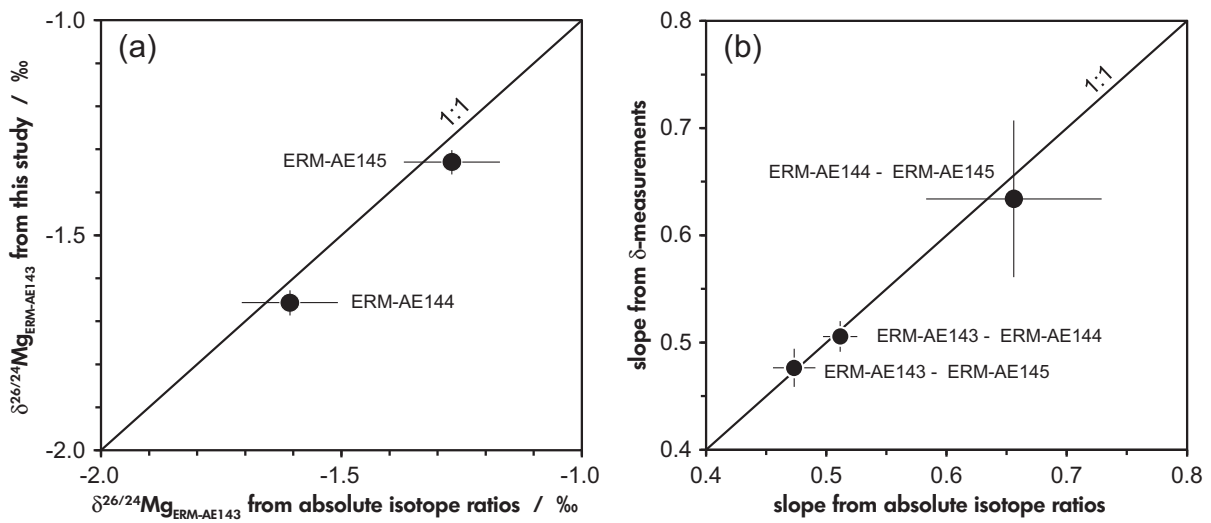


**Figure 3.** Comparison of (a) isotope  $\delta$ -values and (b)  $\theta_{\text{app}}$  or  $S$ -values (slopes in three-isotope space from unrelated samples) from measurement (this study) and calculated from absolute isotope ratios (Vogl *et al.* 2016). The slopes of the pairs ERM-AE143-ERM-AE144 and ERM-AE143-ERM-AE145 are  $S$ -values (materials are unrelated); the slope of the pair ERM-AE144-ERM-AE145 is denoted  $\theta_{\text{app}}$  (materials are related). Within their uncertainties, all results are identical. Uncertainties on  $\delta$ -value measurements are smaller than symbol size; uncertainties on  $\delta$ -values determined from absolute isotope ratios are  $\leq 0.15\text{‰}$  for  $\delta^{26/24}\text{Mg}$ . Uncertainties on slopes are estimated from Tatzel *et al.* (2019).

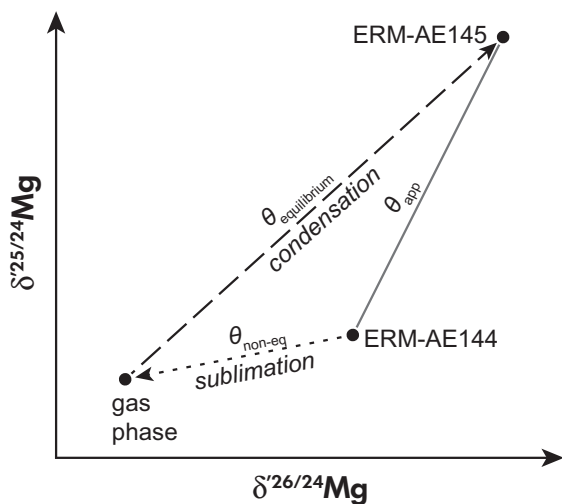


**Figure 4.** Schematic representation of the fractionation history of ERM-AE145 in three-isotope space. A two-step reaction results in a  $\theta_{\text{app}}$ -value  $> \theta_{\text{equilibrium}}$ . Supposedly, high-vacuum sublimation (of ERM-AE144; educt) is a non-equilibrium process that enriched light isotopes in the gas phase. Subsequent condensation of Mg presumably followed an equilibrium process  $\theta_{\text{equilibrium}}$  and lead to an enrichment of heavier isotopes in ERM-AE145.

Also, the slopes in three-isotope space, that is, the difference quotient of linearised  $\delta^{25/24}\text{Mg}$  and  $\delta^{26/24}\text{Mg}$ , yield identical values (Figure 3b). For definitions and explanations of slope,  $\theta$  etc., please refer to the Appendix.

**$^{25}\text{Mg}$  enrichment in ERM-AE145:** Isotope  $\delta$ -value measurements by MC-ICP-MS and isotope  $\delta$ -values calculated from absolute isotope ratios (Vogl *et al.* 2016) show that ERM-AE145 is disproportionately enriched in  $^{25}\text{Mg}$  compared with ERM-AE144 from which it was produced. This phenomenon is entirely unrelated to mass-independent fractionation (MIF) processes, but instead likely results from two subsequent reaction steps that have a different sign of isotope fractionation and different, purely mass-dependent triple isotope fractionation exponents  $\theta$  (equivalent to the exponent  $\beta$  in Young *et al.* 2002) (Figure 4). Two prominent end-member cases calculated based on the quantum mechanical properties of Mg isotopes are presented by  $\theta_{\text{equilibrium}} = 0.521$  and  $\theta_{\text{non-equilibrium}} = 0.511$ , respectively (Young *et al.* 2002). Sublimation of ERM-AE144 in high vacuum during the production process (Brandt *et al.* 2016, Vogl *et al.* 2016) likely fractionated Mg isotopes along a shallow slope, presumably  $\theta_{\text{non-equilibrium}}$  of 0.511, that is, the theoretical slope for non-equilibrium isotope fractionation (calculated based on equation 21 in Young *et al.* 2002 with atomic masses of Mg isotopes). From this gas phase,

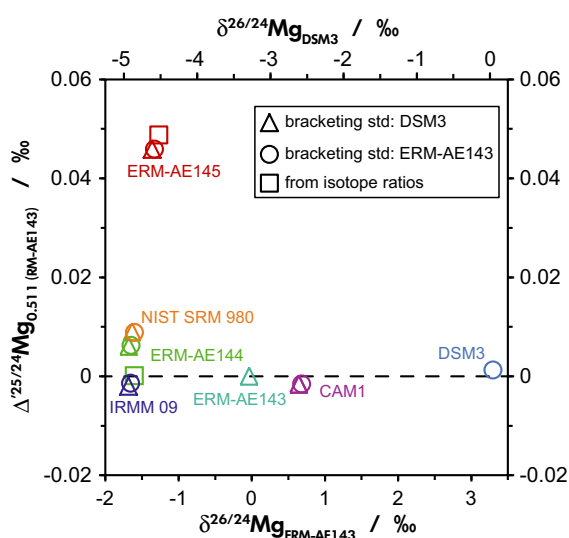


**Figure 5.** Mean  $\Delta^{25/24}\text{Mg}$  values of reference materials measured in this study and from absolute isotope ratio measurements in Vogl *et al.* (2016). Values measured by SSB against ERM-AE143 and DSM3 are shown as circles and triangles, respectively. Values calculated from absolute isotope ratios are shown as squares. All squares and circles refer to the primary x-axis (ERM-AE143 scale) and triangles to the secondary x-axis (DSM3 scale).  $\Delta'$ -values are referenced to a line with a slope of 0.511 originating in ERM-AE143. Samples measured vs. DSM3 are referenced to the same fractionation line, that is, by adding the  $\Delta^{25/24}\text{Mg}$  offset between DSM3 and ERM-AE143 of 0.0013‰.

enriched in the light Mg isotopes, Mg was condensed onto a cooling block made of copper (Brandt *et al.*, 2016). During condensation, Mg isotopes likely fractionated in equilibrium and thus along a steeper slope in three-isotope space, possibly along a slope of 0.521 ( $\theta_{\text{equilibrium}}$ ; calculated based on equation 15 in Young *et al.* (2002) with atomic masses of Mg isotopes). Non-quantitative Mg transfer from the gas phase to the condensed phase is indicated by the experimental magnesium recovery of  $\approx 97\%$  (Brandt *et al.* 2016) and led to a depletion of light isotopes during the condensation process. Hence, the resulting isotope composition of the product ERM-AE145 is enriched in  $^{25}\text{Mg}$  relative to the educt ERM-AE144 as reflected in the apparent  $\theta$ -value,  $\theta_{\text{app}}$ , of  $0.636 \pm 0.073$  ( $k = 2$ ) (Figure 4). The uncertainty on this value (estimate from Tatzel *et al.* 2019) is comparably high due to the low isotopic difference between educt and final product of 0.32‰ for the  $\delta^{26/24}\text{Mg}$ .

**Quantification of  $^{25}\text{Mg}$  isotope enrichment in ERM-AE145:** The  $^{25}\text{Mg}$ -enrichment can be quantified by the linearised isotopic difference  $\Delta^{y/x}E$  between a sample and a reference line, that is, the difference between the measured  $\delta^{y/x}E$  and the  $\delta^{y/x}E$  predicted from the measured  $\delta^{z/x}E$  based on an assumed slope and y-intercept of a reference line in the three-isotope space (where  $x$ ,  $y$  and  $z$  are the low, intermediate and high-mass isotopes of an element  $E$ , respectively). As reference line for Mg isotope analysis, we use the slope of 0.511 originating in ERM-AE143, which was used for SSB measurements. All  $\delta$ -values measured against DSM3 were re-calculated to the same line by adding the measured offset in  $\Delta^{25/24}\text{Mg}$  of

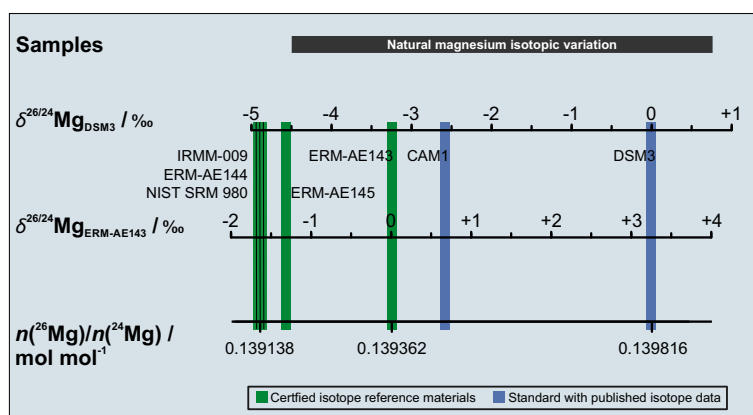


**Figure 6.** New situation for Mg isotope ratios and  $\delta$ -scale measurements as achieved by the presented intercalibration study.

0.0013‰ between DSM3 and ERM-AE143 (mean value from measurements in this study). All these  $\Delta^{25/24}\text{Mg}$ -values are compiled in Figure 5.

## Conclusions

In order to establish SI traceability and the comparability between different Mg  $\delta$ -scales, a magnesium isotope intercomparison study was carried out involving all currently available Mg iRMs and artefact standards with natural-like isotope compositions. Within this intercomparison sufficiently low expanded measurement uncertainties of less than 0.03‰ for the  $\delta^{25/24}\text{Mg}$  values and less than 0.04‰ for the  $\delta^{26/24}\text{Mg}$  values have been achieved. This and the here presented data allow any laboratory to use any of these standards for their research and transfer the obtained  $\delta$ -values into any other scale. This new situation is visualised in Figure 6. Nevertheless, it is recommended to keep the established DSM3 scale and anchor it with ERM-AE143 at -1.681‰ for  $\delta^{25/24}\text{Mg}_{\text{DSM3}}$  and -3.284‰ for  $\delta^{26/24}\text{Mg}_{\text{DSM3}}$  with an associated uncertainty equal to zero. Consequently, an expanded measurement uncertainty of 0.021‰ for the  $\delta^{25/24}\text{Mg}$  value and 0.027‰ for the  $\delta^{26/24}\text{Mg}$  value results for the origin of the scale realised by DSM3.

Additionally, the resulting  $\delta$ -values of ERM-AE143, ERM-AE144 and ERM-AE145 have been checked against the absolute isotope ratios from the certification and perfect agreement was found. For ERM-AE145 and ERM-AE144, which are product and educt of a sublimation–condensation process, an apparent triple isotope fractionation exponent  $\theta_{\text{app}} = 0.636 \pm 0.073$  ( $k = 2$ ), which is outside the range of the theoretical values for non-equilibrium and equilibrium fractionation, has been determined and conclusively explained.

## Acknowledgements

D. Becker and M. Koenig, both BAM, are acknowledged for assistance with the preparation and shipment of the samples. J. Schlegel and J. Buhk are acknowledged for laboratory support at GFZ and F. von Blanckenburg and the Helmholtz Association are thanked for infrastructure support at GFZ. None of the authors have a conflict of interest to declare.

## Data availability statement

The data that support the findings of this study are available in the supplementary material of this article.

## References

**An Y. and Huang F. (2014)**

A review of Mg isotope analytical methods by MC-ICP-MS. *Journal of Earth Science*, 25, 822–840.

**BAM (2018a)**

Certificate of analysis ERM-AE143 Mg in nitric acid (2%, w/w). **Bundesanstalt für Materialforschung und -prüfung (BAM)**. <https://rrr.bam.de/RRR/Navigation/EN/Reference-Materials/reference-materials.html> (last accessed 11/12/2019).

**BAM (2018b)**

Certificate of analysis ERM-AE144 Mg in nitric acid (2%, w/w). **Bundesanstalt für Materialforschung und -prüfung (BAM)**. <https://rrr.bam.de/RRR/Navigation/EN/Reference-Materials/reference-materials.html> (last accessed 11/12/2019).

**BAM (2018c)**

Certificate of analysis ERM-AE145 Mg in nitric acid (2%, w/w). **Bundesanstalt für Materialforschung und -prüfung (BAM)**. <https://rrr.bam.de/RRR/Navigation/EN/Reference-Materials/reference-materials.html> (last accessed 11/12/2019).

**Bizzarro M., Paton C., Larsen K., Schiller M., Trinquier A. and Ulfbeck D. (2011)**

High-precision Mg-isotope measurements of terrestrial and extra-terrestrial material by HR-MC-ICPMS-implications for the relative and absolute Mg-isotope composition of the bulk silicate Earth. *Journal of Analytical Atomic Spectrometry*, 26, 565–577.

**Bolou-Bi E.B., Vigier N., Brenot A. and Poszwa A. (2009)**

Magnesium isotope compositions of natural reference materials. *Geostandards and Geoanalytical Research*, 33, 95–109.

**Brand W.A., Coplen T.B., Vogl J., Rosner M. and Prohaska T. (2014)**

Assessment of international reference materials for isotope-ratio analysis (IUPAC Technical Report). *Pure and Applied Chemistry*, 86, 425–467.

**Brandt B., Vogl J., Noordmann J., Kaltenbach A. and Rienitz O. (2016)**

Preparation and characterization of primary magnesium mixtures for the *ab initio* calibration of absolute magnesium isotope ratio measurements. *Journal of Analytical Atomic Spectrometry*, 31, 179–196.

**Catanzaro E., Murphy T., Garner E. and Shields W. (1966)**

Absolute isotopic abundance ratios and atomic weight of magnesium. *Journal of Research of the National Institute of Standards and Technology*, 70A, 453.



## references

---

### CCQM (2013)

CCQM Guidance note: Estimation of a consensus KCRV and associated degrees of equivalence. CCQM/13-22. [https://www.bipm.org/cc/CCQM/Allowed/19/CCQM13-22\\_Consensus\\_KCRV\\_v10.pdf](https://www.bipm.org/cc/CCQM/Allowed/19/CCQM13-22_Consensus_KCRV_v10.pdf) (last accessed 11/12/2019).

### Foster G.L., Pogge von Strandmann P.A.E. and Rae J.W.B. (2010)

Boron and magnesium isotopic composition of seawater. *Geochemistry Geophysics Geosystems*, 11, 1–10.

### Galy A., Yoffe O., Janney P.E., Williams R.W., Cloquet C., Alard O., Halicz L., Wadhwa M., Hutcheon I.D., Ramon E. and Carignan J. (2003)

Magnesium isotope heterogeneity of the isotopic standard SRM980 and new reference materials for magnesium-isotope-ratio measurements. *Journal of Analytical Atomic Spectrometry*, 18, 1352–1356.

### Geilert S., Vogl J., Rosner M., Voerkelius S. and Eichert T. (2015)

Boron isotope fractionation in bell pepper. *Mass Spectrometry and Purification Techniques*, 1, 1.

### GeoReM (2019)

Max-Planck-Institut für Chemie, Mainz. <http://georem.mpc-h-mainz.gwdg.de> (last accessed 11/12/2019).

### IRMM (2018)

Certificate of analysis IRMM-009 Mg in 0.2 M HNO<sub>3</sub>. Joint Research Centre. <https://crm.jrc.ec.europa.eu/p/40454/40476/By-application-field/Stable-isotopes/IRMM-009-Mg-isotopic-nitrate-solution/IRMM-009> (last accessed 11/12/2019).

### ISO (2010)

Conformity assessment - General requirements for proficiency testing (ISO/IEC 17043:2010). International Organization for Standardization (Geneva). <https://www.iso.org/> (last assessed 05/05/2020)

### ISO (2016)

General requirements for the competence of reference material producers (ISO 17034:2016). International Organization for Standardization (Geneva). <https://www.iso.org/> (last accessed 11/12/2019).

### JCGM 100:2008 (2008)

Evaluation of measurement data – Guide to the expression of uncertainty in measurement. <http://www.bipm.org/en/publications/guides/> (last accessed 11/12/2019).

### NIST (1967)

Certificate of analysis SRM 980 isotopic standard for magnesium. National Institute of Standards and Technology (Gaithersburg, USA). <https://www-s.nist.gov/srmors/certificates/980.pdf> (last accessed 11/12/2019).

### Ling M.-X., Sedaghatpour F., Teng F.-Z., Hays P.D., Strauss J. and Sun W. (2011)

Homogeneous magnesium isotopic composition of seawater: An excellent geostandard for Mg isotope analysis. *Rapid Communications in Mass Spectrometry*, 25, 2828–2836.

### Metrodata (2019)

GUM Workbench version 2.4.1.375 – Software for calculating the measurement uncertainty. Metrodata GmbH (Braunschweig). <http://www.metrodata.de> (last accessed 11/12/2019).

### Pogge von Strandmann P.A.E., Elliott T., Marshall H.R., Coath C., Lai Y.J., Jeffcoate A.B. and Ionov D.A. (2011)

Variations of Li and Mg isotope ratios in bulk chondrites and mantle xenoliths. *Geochimica et Cosmochimica Acta*, 75, 5247–5268.

### Pokharel R., Gerrits R., Schuessler J.A., Floor G.H., Gorbushina A.A. and von Blanckenburg F. (2017)

Mg isotope fractionation during uptake by a rock-inhabiting, model microcolonial fungus *Knufia petricola* at acidic and neutral pH. *Environmental Science and Technology*, 51, 9691–9699.

### Pokharel R., Gerrits R., Schuessler J.A., Frings P.J., Sobotka R., Gorbushina A.A. and von Blanckenburg F. (2018)

Magnesium stable isotope fractionation on a cellular level explored by cyanobacteria and black fungi with implications for higher plants. *Environmental Science and Technology*, 52, 12216–12224.

### Rosner M., Pritzkow W., Vogl J. and Voerkelius S. (2011)

Development and validation of a method to determine the boron isotopic composition of crop plants. *Analytical Chemistry*, 83, 2562–2568.

### Schuessler J.A., von Blanckenburg F., Bouchez J., Uhlig D. and Hewawasam T. (2018)

Nutrient cycling in a tropical montane rainforest under a supply-limited weathering regime traced by elemental mass balances and Mg stable isotopes. *Chemical - Geology*, 497, 74–87.

### Shalev N., Farkaš J., Fietzke J., Novák M., Schuessler J.A., Pogge von Strandmann P.A.E. and Törber P.B. (2018)

Mg isotope interlaboratory comparison of reference materials from Earth-surface low-temperature environments. *Geostandards and Geoanalytical Research*, 42, 205–221.

### Tatzel M., Vogl J., Rosner M., Tütken T. and Henehan M. (2019)

Triple isotope fractionation exponents of elements measured by MC-ICP-MS – An example of Mg. *Analytical Chemistry*, 91, 14314–14322.

### Teng F.-Z. and Yang W. (2014)

Comparison of factors affecting the accuracy of high-precision magnesium isotope analysis by multi-collector inductively coupled plasma-mass spectrometry. *Rapid Communications in Mass Spectrometry*, 28, 19–24.

### Teng F.-Z., Li W.-Y., Ke S., Yang W., Liu S.-A., Sedaghatpour F., Wang S.-J., Huang K.-J., Hu Y., Ling M.-X., Xiao Y., Liu X.-M., Li X.-W., Gu H.-O., Sio C.K., Wallace D.A., Su B.-X., Zhao L., Chamberlin J., Harrington M. and Brewer A. (2015)

Magnesium isotopic compositions of international geological reference materials. *Geostandards and Geoanalytical Research*, 39, 329–339.



## references

---

**Teng F.-Z. (2017)**

Magnesium isotope geochemistry. *Reviews in Mineralogy and Geochemistry*, 82, 219–287.

**Uhlig D., Schuessler J.A., Bouchez J.L., Dixon J. and von Blanckenburg F. (2017)**

Quantifying nutrient uptake as driver of rock weathering in forest ecosystems by magnesium stable isotopes. *Biogeochemistry*, 14, 3111–3128.

**Vogl J., Pritzkow W. and Klingbeil P. (2004)**

The need for new Sr-traceable magnesium isotopic reference materials. *Analytical and Bioanalytical Chemistry*, 380, 876–879.

**Vogl J., Rosner M. and Pritzkow W. (2013)**

The need for new isotope reference materials. *Analytical and Bioanalytical Chemistry*, 405, 2763–2770.

**Vogl J., Brandt B., Noordmann J., Rienitz O. and Malinovsky D. (2016)**

Characterization of a series of absolute isotope reference materials for magnesium: *Ab initio* calibration of the mass spectrometers, and determination of isotopic compositions and relative atomic weights. *Journal of Analytical Atomic Spectrometry*, 31, 1440–1458.

**Young E.D., Galy A. and Nagahara H. (2002)**

Kinetic and equilibrium mass-dependent isotope fractionation laws in nature and their geochemical and cosmochemical significance. *Geochimica et Cosmochimica Acta*, 66, 1095–1104.

## Supporting information

---

The following supporting information may be found in the online version of this article:

Table S1. Reported  $\delta^{25/24}\text{Mg}_{\text{ERM-AE143}}$  values with their precision and their associated uncertainty listed first by institute and second by sample in alphabetical order.

Table S2. Reported  $\delta^{26/24}\text{Mg}_{\text{ERM-AE143}}$  values with their precision and their associated uncertainty listed first by institute and second by sample in alphabetical order.

Appendix S1. Terminology.

This material is available from: <http://onlinelibrary.wiley.com/doi/10.1111/ggr.12327/abstract> (This link will take you to the article abstract).

## Appendix A

---

To avoid misunderstanding and/or ambiguity, the definitions of some lesser-known quantities within this article are given in the following.

$\alpha^{(y/x)E}$ : Isotope fractionation factor describes the isotope

fractionation in reaction A-B  $\alpha_{A-B}^{y,z/x} = \frac{\left(\frac{n^{(y,z)E}}{n^{(x)E}}\right)_A}{\left(\frac{n^{(y,z)E}}{n^{(x)E}}\right)_B}$  with the

relationship in three-isotope systems  $\alpha_{A-B}^{y/x} = \left(\alpha_{A-B}^{z/x}\right)^{\theta}$

$\theta$ : Triple isotope fractionation exponent, sometimes represented by  $\beta$ , is the slope of the fractionation line between an educt and a product in a three-isotope diagram of linearised delta values  $\delta^{y/x}E$  versus  $\delta^{z/x}E$ , for example,  $\delta^{25/24}\text{Mg}$  versus  $\delta^{26/24}\text{Mg}$ .

$\theta_{\text{app}}$ : Apparent triple isotope fractionation exponent

$\theta_{\text{equilibrium}}$ : Triple isotope fractionation exponent of an equilibrium process, for example, for magnesium 0.521

$\theta_{\text{non-equilibrium}}$ : Triple isotope fractionation exponent of a non-equilibrium process, for example, for magnesium 0.511

S-value: Slope of the linear regression line from unrelated samples in a three-isotope diagram

$\Delta^{y/x}E$ : Linearised isotopic difference  $\Delta^{y/x}E$  between a sample and a reference line, that is, the difference between the measured  $\delta^{y/x}E$  and the  $\delta^{y/x}E$  predicted from the measured  $\delta^{z/x}E$  based on an assumed slope and y-intercept of a reference line

